Swansea University
Prifysgol Abertawe

Cronfa
Setting Research Free

Cronfa - Swansea University Open Access Repository

This is an author produced version of a paper published in :
Renewable Energy

Cronfa URL for this paper:
http://cronfa.swan.ac.uk/Record/cronfa20864

Paper:
Fairley, I., Ahmadian, R., Falconer, R., Willis, M. & Masters, I. (2014). The effects of a Severn Barrage on wave conditions in the Bristol Channel. *Renewable Energy, 68*, 428-442.

http://dx.doi.org/10.1016/j.renene.2014.02.023

This article is brought to you by Swansea University. Any person downloading material is agreeing to abide by the terms of the repository licence. Authors are personally responsible for adhering to publisher restrictions or conditions. When uploading content they are required to comply with their publisher agreement and the SHERPA RoMEO database to judge whether or not it is copyright safe to add this version of the paper to this repository.
http://www.swansea.ac.uk/iss/researchsupport/cronfa-support/

Elsevier Editorial System(tm) for Renewable Energy
Manuscript Draft

Manuscript Number: RENE-D-13-00737R1

Title: The effects of a Severn Barrage on wave conditions in the Bristol Channel

Article Type: Original Research Paper

Keywords: tidal barrage; wave-current interaction; SWAN; marine energy; coastal hydrodynamics

Corresponding Author: Dr. Iain Alastair Fairley, Ph.D.

Corresponding Author's Institution: Swansea University

First Author: Iain Fairley

Order of Authors: Iain Fairley; Reza Ahmadian; Roger Falconer; Miles Willis; Ian Masters

Abstract: The study investigates the impact that construction of a Severn Barrage in the Severn Estuary, on the west coast of the UK, might have on local wave conditions. Implementation of a barrage will impact on tidal currents and water elevations in the wider region. There is strong tidal modulation of wave conditions under the natural regime and therefore barrage-induced changes to tidal conditions could affect wave modulation in the region. This paper uses Swan, an open source 3rd generation spectral wave model, to investigate the possible impacts of construction of a barrage on tidal modulation of the wave conditions. It is found that current variations, rather than water level variations, are the dominant factor in tidal modulation of wave conditions. Barrage implementation does not substantially change the modulation of the wave period or direction. However, barrage implementation does affect the tidal modulation of wave heights in the area of interest. The tidal modulation of the wave heights is generally reduced compared to the natural case; the peaks in the wave heights on an incoming tide are slightly lowered and there is lesser attenuation in wave heights on the outgoing tide. This modulation leads to net changes in the wave heights over one tidal cycle. For all of the tested wave conditions, this net change is small for the majority of the tested domain, namely to within ±5% of the no barrage case. There are some areas of greater change, most notably larger net increases in the wave heights near the North Somerset coast where the post construction net wave height increase over a tidal cycle approach 20% of the pre-construction conditions. These changes do not impact coastal flooding because the wave height increase is not co-incident with high tide. Importantly, the maximum wave height is not increased and thus the likelihood of extreme events is not increased. The area of greatest reduction is between Swansea and Porthcawl. Changes over a neap tidal cycle show similar patterns of net change, but the modulation over the tidal cycle is different; primarily the magnitude of modulation is half that for the spring tide case and the shape is altered in some locations.

The effects of a Severn Barrage on wave conditions in the Bristol Channel

Fairley, I.[1,#], Ahmadian, R.[2], Falconer R.A[2], Willis, M.R.[1], Masters, I[1].

1. Marine Energy Research Group, College of Engineering, Swansea University, Swansea, SA2 8PP, UK.

2. Hydro-environmental Research Centre,School of Engineering, Cardiff University, Cardiff, CF24 3AA, U.K.

#. Corresponding author: Dr. Iain Fairley,

Email: i.a.fairley@swansea.ac.uk

Tel: +44 (0)1792 602326

Abstract

The study investigates the impact that construction of a Severn Barrage in the Severn Estuary, on the west coast of the UK, might have on local wave conditions. Implementation of a barrage will impact on tidal currents and water elevations in the wider region. There is strong tidal modulation of wave conditions under the natural regime and therefore barrage-induced changes to tidal conditions could affect wave modulation in the region. This paper uses Swan, an open source 3rd generation spectral wave model, to investigate the possible impacts of construction of a barrage on tidal modulation of the wave conditions. It is found that current variations, rather than water level variations, are the dominant factor in tidal modulation of wave conditions. Barrage implementation does not substantially change the modulation of the wave period or direction. However, barrage implementation does affect the tidal modulation of wave heights in the area of interest. The tidal modulation of the wave heights is generally reduced compared to the natural case; the peaks in the wave heights on an incoming tide are slightly lowered and there is lesser attenuation in wave heights on the outgoing tide. This modulation leads to net changes in the wave heights over one tidal cycle. For all of the tested wave conditions, this net change is small for the majority of the tested domain, namely to within ±5% of the no barrage case. There are some areas of greater change, most notably larger net increases in the wave heights near the North Somerset coast where the post construction net wave height increase over a tidal cycle approach 20% of the pre-construction conditions. These changes do not impact coastal flooding because the wave height increase is not co-incident with high tide. Importantly, the maximum wave height is not increased and thus the likelihood of extreme events is not increased. The area of greatest reduction is between Swansea and Porthcawl. Changes over a neap tidal cycle show similar patterns of net change, but the modulation over the tidal cycle is different; primarily the magnitude of modulation is half that for the spring tide case and the shape is altered in some locations.

Key words: Tidal barrage, wave-current interaction, SWAN, Marine Energy, Coastal Hydrodynamics

1. Introduction

The Severn Estuary and Bristol Channel has the second largest tidal range in the world and therefore has been the subject of many proposals to generate energy via various marine renewable energy schemes, including tidal barrages. A barrage for the extraction of tidal energy has been proposed by Severn Tidal Power Group between Cardiff and Weston-Super-Mare in the Severn Estuary (Figure 1). The area has a range of coastal environments from low lying dunes to hard cliff regions and is open to storm and swell waves from the Atlantic Ocean. Any change to wave conditions forced by a barrage construction has the potential to affect coastal erosion and coastal flooding in the region, as well as recreational water sports. Beyond being a case study, this paper demonstrates the potential impact of tidal energy extraction on local wave conditions. As more tidal range and tidal stream energy projects are developed, changes to the tidal hydrodynamics over wide spatial areas are possible and the corresponding hydrodynamic impacts [1, 2] need to be investigated further. This may mean there are associated changes to the wave climate, as well as the tidal characteristics. Presently, given only a few individual devices have been deployed, this has not been considered, but as larger scale tidal stream array developments take place such cumulative impacts must be considered.

1.1 Tidal energy and the Severn Estuary

Tidal range energy generation schemes can be categorised into tidal lagoons and tidal barrages. To date, barrages have only been deployed in a few areas: a 240MW barrage in Brittany, France [3], a 20MW facility in the Bay of Fundy [4], and other developments in Russia and Korea. A review of existing and potential barrage sites is given by O Rourke *et al* [5]. Tidal range schemes are currently receiving less research attention than tidal stream energy generation [6]; however there is the potential for much larger energy returns. Given the huge potential of tidal barrages, it is vital to maintain research focus to fully understand the impact of such schemes.

The Severn Estuary has a peak mean spring tidal range of 14m, one of the largest ranges in the world. Therefore, proposals to generate electricity via a barrage have been considered for many years. It is recognised that a barrage could greatly contribute to renewable energy supplies within the UK; recent reports have suggested that, based on a Cardiff-Weston proposal (Figure 1), it could generate 17 TWhr/Year, which corresponds to 5% of the UK's energy supply [7]. As reported by the Severn Tidal Power Group (STPG), EP57 report [1], the barrage would include: 166 sluice gates and 216 × 9 m diameter bulb turbines, each producing a peak output of 40 MW. Implementation of a Severn Barrage could have fulfilled a significant portion of the UK Government's 2020 carbon emission reduction targets. Furthermore, major infrastructure projects, such as the barrage, have the potential to re-generate the economy of entire regions [7,8,9]. Equally, improved transport links making use of a barrage may bring additional prosperity to regions such as Wales and the South West. Thus, it can be seen that the concept of a Severn Barrage is attractive from an engineering and economical perspective, given both the energy and current financial crisis. Furthermore, the barrage can reduce flood risk upstream of the barrage for both the existing and future

climatic conditions, as well as reducing suspended sediment levels and consequently increasing light penetration in the estuary [10]. However, inter-tidal mudflats in the estuary would be reduced due to increased low water levels [11].

Balancing the potential benefits of such a proposal is the potential for adverse environmental impacts. A significant amount of research effort has gone into understanding the hydrodynamic impacts (currents and water levels) of the Severn barrage [12, 13], and some consideration of the effects on the water quality [14], birdlife [15, 16], fish [17] and other environmental considerations [18-22]. However, one area that has received little consideration is the possible impact of the Severn barrage on the wave conditions in the Severn Estuary. The Severn barrage could affect wave conditions in two ways. To the east (upstream) of the barrage, the barrage will directly block swell and wind waves incident from the Atlantic and the only waves in the region will be fetch limited wind waves. To the west (downstream) of the barrage, in the outer estuary, changes to tidal elevations and currents caused by a barrage implementation may modulate the incoming wave field via wave-current interactions. This paper therefore addresses the downstream (up-wave) impact of a barrage. Changes to the wave climate in the outer estuary could alter the coastal sediment transport pathways, with implications for coastal engineering and management. It could also impact on recreational sea use. The seas around South Wales and North Devon are popular surfing destinations with an associated tourist industry; any perceived degradation of surfing conditions caused by a barrage are likely to result in strong opposition from these stakeholders.

1.2 Wave-current interaction in the Severn Estuary and Bristol Channel

Wave-current interaction is a well-researched and documented process [23], with both currents affecting waves and waves affecting currents. In this study only the effect of currents on waves is considered. The most extreme case of wave-current interaction is wave blocking. This phenomenon occurs when waves are incident to an opposing current, with the same velocity as the intrinsic wave group velocity, and thus the energy transport referenced to the fixed bed reduces to zero. Additionally, waves can break against an opposing current, or undergo dissipation in the fluid body and wave boundary layers. Wave trains are doppler shifted, whilst travelling in the presence of following or opposing currents which can influence wave spectra. Equally important are current-induced refraction of wave fields. Depth limited breaking and wave dissipation may also be affected, given changes to the tidal range. This may be an important process in the study region, due to the presence of several large and shallow sandbanks.

The large tidal range in the Bristol Channel means that there is a significant wave current interaction and tidal modulation of the wave field. This modulation can be observed in wave buoy records within the estuary. Figure 2 demonstrates observed tidal modulation of the wave parameters recorded at Scarweather Sands (see Figure 1), between 31/03/2010 and 31/01/2012 at ½ hourly intervals. All parameters show a distinct peak at the semi-diurnal tidal frequency (1.936 cycles/day).

Researchers at the Hydro-environmental Research Centre at Cardiff University have developed an open source model, namely DIVAST, that solves the shallow water equations

via a finite volume technique; its architecture and use has been described in several papers [10, 13, 24, 25]. The model has been set up for the Severn Estuary and Bristol Channel and used to investigate the hydrodynamic impact of a barrage implementation [11,13,14, 25, 26], Xia *et al* [13] suggest that current velocities and maximum water levels will both reduce. The DIVAST model shows that mean current reductions with the barrage in place are in the region 0.5 m/s and tidal elevations upstream of the barrage will be reduced by between 0.5m and 1.5m.

Given the observed tidal modulation of the wave height (Figure 2) and the previously predicted changes to the tidal hydrodynamics, one can expect that implementation of a Severn barrage will affect the incident wave climate to some extent. It is hypothesized that the tidal modulation of the wave climate will be reduced with greater parity between conditions on the flood and ebb tides for the case with a barrage in place. If such changes occur, there could be implications for coastal sediment transport, flood risk and local biology. This paper uses the open source 3rd generation wave model, Swan, to test and verify the stated hypothesis, although it is found the magnitude of change is small. The paper is organised as follows: firstly the methodology is discussed, paying particular attention to the alterations to the Swan code to cater better for wave-current interaction; secondly a series of characteristic wave conditions are tested for both spring and neap tides, with and without the barrage in place; finally some comments are made on the implications of the projected changes.

2. Methodology

Water levels and (*u,v*) current velocities output from DIVAST were used to force a Swan 3rd generation spectral wave model of the outer Severn Estuary. Wave boundary conditions were taken from the resultant wave output of the 2nd generation Met Office wave model [27] at a point located in the centre of the wave boundary at 51.25N 4.46W. The Swan model was validated against a wave buoy record and then run with test wave conditions, derived from the Met Office data, to investigate the impact of a barrage construction on the wave conditions. Both spring and neap tide tests were conducted, as were tests with water levels only, to verify the importance of currents given the shallow bathymetry of the region.

2.1 DIVAST Hydrodynamic model

The western limit of the hydro-environmental model domain for this study was selected to be at the outer Bristol Channel and the domain was extended to the River Severn tidal limit close to Gloucester at the Eastern end of the estuary, as shown in Figure 1. The domain covers an area which is approximately 5700 km^2 and is 200km long.

A depth integrated 2D DIVAST model was implemented to simulate the hydrodynamic process across the model domain. This was due to the mainly horizontal nature of the flow in the region, without any substantial sign of stratification and vertical velocities [13, 26, 28 - 31].

The governing depth-integrated shallow water equations and the numerical solution schemes implemented in the model are outlined below. More details of the model can be found in Xia *et al.* [13, 26].

The general conservative form of the shallow water equations can be written as:

$$\frac{\partial U}{\partial t}+\frac{\partial E}{\partial x}+\frac{\partial G}{\partial y}=\frac{\partial \tilde{E}}{\partial x}+\frac{\partial \tilde{G}}{\partial y}+S \tag{7}$$

where U = vector of conserved variables; E and G = convective flux vectors of flow in the x and y directions, respectively; $\tilde{E}$ and $\tilde{G}$ = the turbulent stress related diffusive vectors in the x and y directions, respectively; and S = source term including: the Coriolis force, bed friction and bed slope. Each of these terms can be expressed in more detail as below:

$$U=\begin{bmatrix} h \\ hu \\ hv \end{bmatrix},\ E=\begin{bmatrix} hu \\ hu^2+\frac{1}{2}gh^2 \\ huv \end{bmatrix},\ G=\begin{bmatrix} hv \\ huv \\ hv^2+\frac{1}{2}gh^2 \end{bmatrix},\ \tilde{E}=\begin{bmatrix} 0 \\ \tau_{xx} \\ \tau_{yx} \end{bmatrix},$$

$$\tilde{G}=\begin{bmatrix} 0 \\ \tau_{xy} \\ \tau_{yy} \end{bmatrix},\qquad S=\begin{bmatrix} q_s \\ +hfv+gh\left(S_{bx}-S_{fx}\right) \\ -hfu+gh\left(S_{by}-S_{fy}\right) \end{bmatrix} \tag{8}$$

where h = total water depth (m); u, v = depth-averaged velocities (m/s) in the x and y directions, respectively; g = gravitational acceleration (m/s^2); *f* = Coriolis acceleration due to the earth's rotation, in which $f=2\omega\sin\emptyset$ (rad/s), ω = earth's angular velocity (7.29×10^{-5} rad/s) and $\emptyset$ = latitude of study domain (rad); S_{bx} and S_{by} = bed slopes in the x and y directions, respectively (dimensionless); S_{fx} and S_{fy} = friction slopes in the x and y directions (dimensionless), respectively; q_s = source (or sink) discharge per unit area (m/s) and τ_{xx}, τ_{xy}, τ_{yx} and τ_{yy}= components of the turbulent shear stress over the plane (N/m^2).

The seaward model boundary is a water level boundary, with data acquired from the Proudman Oceanographic Laboratory (POL) Irish Sea model as shown in Figure 1. An average river discharge was used for River Severn inflow at the Eastern boundary and source points as shown in [9, 23, 32]. A triangular unstructured mesh was implemented in this study in order to acquire more accurate predictions in the area of interest, e.g. vicinity of the barrage. The model included 37,423 cells and higher resolution was used around the barrage site and the deep channels. The barrage was modelled using the domain decomposition technique. Using this technique, two sub models were linked via internal boundaries, namely turbines and sluice gates. More details on modelling the barrage and sluice gates can be found in [13, 14].

A cell-centred finite volume method was implemented in this model, with the average values of the conserved variables being calculated at the centre of the cells. The flux at the interface of two adjacent cells was considered as a locally one-dimensional problem perpendicular to the interface. The volume flux between neighbouring cells was obtained using the Monotone Upstream Scheme for Conservation Laws (MUSCL) being implemented in the current study [13, 26]. The second order accuracy in time, as well as space, was accomplished by application of the predictor-corrector time stepping.

In order to eradicate the reflection of waves generated inside the domain at the seaward boundary, the state variables at the seaward boundary were calculated using a non-reflecting boundary procedure based on the theory of characteristics [33]. More details of the numerical solution of the governing equations and model details can be found in [13, 26].

2.1.1 DIVAST Validation

The Severn Estuary model used in this study has been extensively calibrated and validated previously; the reader is directed to Xia *et al* [13] for a full description of these validations. For completeness, a typical model validation is presented in Figure 3. It can be seen that modelled water levels, current speeds and directions all fit well with observations. . A brief summary of the key DIVAST model parameters is given in Table 1. More details of the model can be found in [13, 26].

2.1.2 DIVAST outputs used as wave model forcing

Calibrated and validated DIVAST model outputs are available over a spring neap cycle between 05:00 on 21/07/2001 and 05:00 on 02/08/2001. The entire period is used for validation of the wave model and subsets used for spring and neap tide conditions to test differing wave conditions. The spring tide period was between 01:30 on 23/07/2001 and 08:30 on 24/07/2001, the neap tide period was between 07:15 on 29/07/2001 and 15:15 on 30/07/2001 (Figure 4). Changes to current velocities are more striking than changes to water levels. Example current velocities from one spring tidal cycle at high water, mid-ebb, low water, and mid flood are shown for both pre- and post-barrage scenarios in Figure 5. The impact of the barrage in reducing tidal currents downstream of the barrage can be clearly seen. Particularly large current reductions are noticeable in the portion of the estuary north of Minehead. The low tide current in the deep channel south of Barry is also reduced with barrage implementation.

2.2 Swan Wave Model

The spectral wave model Swan is regularly used in academia; its architecture, features and validation have been well documented in the literature [35-36]. The model is regularly used in the renewable energy field, where it is often used for wave energy resource description (e.g. [37-39]) and wave farm impact studies (e.g. [40]). Swan computes the wave action density N using the action balance equation [43]:

$$\frac{\partial N}{\partial t} + \nabla_{x,y} \cdot \left[\left(\vec{c_g} + \vec{U}\right)N\right] + \frac{\partial}{\partial \theta}(c_\theta N) + \frac{\partial}{\partial \sigma}(c_\sigma N) = \frac{S_{tot}}{\sigma} \quad (1)$$

where:

$$S_{tot} = S_{in} + S_{wc} + S_{quad} + S_{bot} + S_{brk} + S_{triad} \quad (2)$$

In Equation 1, the terms on the left hand side describe, in order: the change in wave action over time ($\frac{\partial N}{\partial t}$), geographical propagation of wave action depending on wave group velocity

(C_g) and the current velocity (U), depth and current-induced refraction ($\frac{\partial}{\partial\theta}(c_\theta N)$) and shifting of the relative radian frequency ($\frac{\partial}{\partial\sigma}(c_\sigma N) = \frac{S_{tot}}{\sigma}$). The term on the right hand side incorporates the physical processes that generate, dissipate or redistribute the wave energy. These physical processes are given in equation 2, where: S_{in} is the wind generated energy, S_{wc} is the energy lost by white-capping, S_{quad} is the redistribution of energy by nonlinear quadruplet wave-wave interactions, S_{bot} is the dissipation of wave energy due to bottom friction, S_{brk} is the depth-induced breaking, and S_{triad} is the nonlinear triad re-distribution of wave energy.

It is recognised that spectral wave models can have some difficulty in accurately representing wave–current interaction. Under blocking conditions, theory suggests that wave heights would tend to infinity for monochromatic conditions, which is clearly unrealistic. Additionally, comparisons with measurements have shown that wave heights are over estimated by Swan using standard settings for an opposing current [41-43], although wave heights in a following current are well predicted [41]. A version of the Swan 40.81, which was modified to model dissipation of waves by currents more accurately, was used in this work. The modifications were implemented by van der Westhuysen to include his work on improved wave-current interactions in Swan [41, 43], a synopsis of which follows below.

2.2.1 Wave-current interaction in SWAN

Wave heights in opposing currents are dissipated via current-induced wave breaking, which can be modelled using a 3rd generation white-capping expression. The default white-capping expression used in Swan is based on the pulse-based model of Hasselman [44], modified by Komen *et al* [45]. Ris and Holthuijsen [37] showed that this expression alone over-predicted wave heights on an opposing current, due to unrealistically high values for the wave steepness being permitted. The inclusion of the bore-based model of Battjes and Janssen [41] for steep breaking waves in deep water was shown to improve the results, although errors in prediction still existed. Chawla and Kirby [42] note the difference between saturated depth limited breaking and the breaking observed in a following current which is weak and non-saturated. This implies that the bore breaker model may not be the most suitable representation of depth-induced breaking. Van der Westhuysen tested the performance of a different saturation-based white-capping expression in predicting wave heights in an opposing current [36, 48]. Van der Westhuysen [43] initially implemented a saturation-based white-capping formulation, based on Alves and Banner [49] and Yan [50], in order to correct the under-prediction of wave period by Swan. The default version of this expression, calibrated for wind growth, over estimates wave heights for an opposing current, similar to the pulse-based model. Van der Westhuysen [41, 43] combines the saturation-based white-capping expression of [48] with an additional term for current-induced white-capping, adding another source term, $S_{wc,curr,}$ to equation 2 to improve the capability of Swan in regions of strong wave-current interaction. The original S_{wc} term from Van der Westhuysen [48] is given as:

$$S_{wc}(\sigma,\theta) = f_{br}(\sigma)S_{dis,break} + [1 - f_{br}(\sigma)]S_{dis,non-break} \quad (3)$$

where f_{br} is a weighting function determining whether dissipation is by breaking or non-breaking, which depends upon the ratio between the spectral saturation and a threshold saturation level. The additional term proposed by Van der Westhuysen [41] for enhanced dissipation by currents follows the form of the $S_{dis,break}$ term in (3), giving:

$$S_{dis,break}(\sigma,\theta) = -C_{ds}\left[\frac{B(k)}{B_r}\right]^{\frac{p}{2}}[\tanh(kd)]^{\frac{2-p}{4}} g^{\frac{1}{2}} k^{\frac{1}{2}} E(\sigma,\theta) \quad (4)$$

The enhanced dissipation is scaled by the normalised propagation speed of the relative radian frequency in frequency space (C_σ/σ) in order to isolate the role of currents in wave steepness and dissipation. The term $[\tanh(kd)]^{\frac{2-p}{4}}$ in equation (4) is neglected as it was found to have relatively minimal effect and a maximum function included to ensure only relative increases in steepness are included in the dissipation. Therefore the term $S_{wc,curr}$ is given by:

$$S_{wc,curr} = -C''_{ds}\, max\left[\frac{C_\sigma(\sigma,\theta)}{\sigma}, 0\right]\left[\frac{B(k)}{B_r}\right]^{\frac{p}{2}} E(\sigma,\theta) \quad (5)$$

where *B(k)* is the spectral saturation and B_r is the threshold saturation which is given by [48] to be $1.75\text{x}10^{-3}$. *P* is a function of the inverse wave age and is given in (6) and the propagation speed of the relative radian frequency, C_σ, is given in (7):

$$p(u_*/c) = 3 + tanh\left[25\left(\frac{u_*}{c} - 0.1\right)\right] \quad (6)$$

$$C_\sigma = \frac{d\sigma}{dt} = \frac{\partial\sigma}{\partial d}\left[\frac{\partial d}{\partial t} + \vec{U}\cdot\nabla_{x,y} d\right] - c_g \cdot \vec{k} \cdot \frac{\partial \vec{U}}{\partial r} \quad (7)$$

where *d* is the water depth and *r* is the space co-ordinate in the direction of propagation. The calibration parameter C''_{ds} is found by van der Westhuysen [43] to be 0.65, based on error optimisation using model runs representing the laboratory flume experiments of Lai *et al* [51] and Suastika *et al* [52].

Van der Westhuysen found that this formulation is suitable for both developed wave fields and young wind-seas and that the formulation better predicts dissipation of wave energy on a counter current [41, 43]. The prediction of wave height on a following current gradient is also well catered for [43].

2.2.2 Wave model set-up

Swan version 40.81 was used for these simulations with all parameters set to the default values as recommended by the manual [53]. The model domain covers the Severn Estuary and Bristol Channel, with the western boundary of the domain towards the outer limit of the Bristol Channel (the red line in Figure 1). The western boundary was selected to be inside the model domain of the hydrodynamic model (which was bounded on the west by the green line in Figure 1) in order to avoid boundary effects from the hydrodynamic model and wave model occurring at the same location. The Eastern boundary of the model was located far enough up the estuary that waves were no longer important. An unstructured mesh (Figure 6) was created using Battri [54], a matlab interface for the Triangle mesh generation

programme [55]. The same bathymetry as used in the DIVAST model was used for the wave model and the currents and water levels were implemented in Swan on a 1km regular grid.

In modelling the barrage, the same grid as the non-barrage case was used. The Swan 'Obstacle' command was used to represent the barrage as a line with a wave transmission co-efficient of 0. It was assumed that the barrage would be designed to have a minimal reflection co-efficient to reduce wave impacts and therefore the reflection co-efficient was set to 0. For simplicity, the barrage was modelled as a straight line in the wave model (the modelling of the barrage in the DIVAST hydrodynamic model is discussed in section 2.1). While this was marginally different to the proposed plans, there was thought to be no significant impact on the resulting findings presented herein.

For each scenario, the model was run in non-stationary mode over three tidal cycles with a time step of 5 minutes and outputs were generated every 10 minutes.

No wind growth was included in any of the simulations. The motivation for this approach was that the bulk of the work focusses on characteristic wave conditions rather than historical time-periods. Therefore including a range of characteristic wind conditions would multiply the number of test cases and obscure the thrust of the results in what is primarily an illustrative study.

2.2.3 Wave model validation

Only one wave buoy was active in the domain during the simulation period, which was temporally constrained by data availability for the hydrodynamic model. Therefore, it was believed that it was more valuable to use the rigorously tested default settings, rather than to calibrate tuneable parameters in the model to one measurement point which might not be representative of the entire domain. Consequently, default settings were used in the model set up and the model was validated against this point before simulations with characteristic wave conditions over spring and neap tides were conducted.

For validation purposes, the wave model was run over eleven days, with wave boundary conditions taken from the UK Met Office 2nd generation wave model. The resultant wave conditions were used from a model output point in the centre of the incident wave boundary at 51.25N 4.46W (Figure 1). Figure 7 shows that the model predicts the magnitude of the wave heights correctly but that the tidal modulation is over predicted by the wave model. Indeed no tidal modulation is observable in the wave buoy, despite being clearly present in other more recent wave buoy records (e.g Cefas Wavenet Scarweather buoy). It is postulated that this disparity could either be due to the lack of wind growth or a lack of sensitivity in the wave buoy. As proof that the model is correctly capturing the tidal modulation, Figure 8 shows a spectral density plot of the modelled data and data collected by a Datawell Waverider at the same location between 2005-2011 as part of the Wavenet project. Given the different time periods and sample periods, the magnitude of spectral density varies between the two records and thus the spectral density was normalised by the maximum spectral density. The shape of the spectral density is not altered by the normalisation and this is similar between the modelled and measured data. Therefore, one can infer that the tidal modulation is similar for both records. In particular, the plot shows that both records have a primary spectral peak at ~1.9 cycles per day, which is the semidiurnal

tidal frequency, and then the relative level between the spectral peak and both the first harmonic and the background level is similar. The model does seem to be over predicting the higher harmonics and exhibiting less noise at the higher frequencies, but both these differences are attributed to the short model run-time and lesser number of samples.

2.2.4 Wave boundary conditions and tests conducted

Wave data for 2000-2008 has been obtained from a Met Office wave model hindcast point in the centre of the Bristol Channel and in the middle of the incident boundary (51.25N 4.46W). These data are displayed in Figure 9. This figure shows a joint probability of occurrence plot for significant wave height and mean wave period. The data are screened such that only waves incident into the channel are considered (20-135 deg N.) These data are used to calculate mean wave conditions and extreme storm conditions. Extreme storm wave conditions were established by identifying the largest wave conditions from the record. The swell wave component of the 2nd generation model was used to determine a swell condition representative of swells for recreational surfing use. This was established by calculating the mean of the swell wave component, where wave heights exceeded 1m (hence being of sufficient height for board riding). The Met Office model used to calculate the boundary conditions did not output the directional spread, D_{spr}, therefore the mean of the Cefas Scarweather Sands wave buoy, 17.5º, was used for this value. These three conditions are shown in Table 2. All conditions were tested on spring tides. Additional simulations were run for mean conditions over a spring tide without currents, over neap tide conditions and over spring tides with differing directional spread.

3. Results

In this section, spatial maps of change across the domain are discussed as are time series extracted at four key points spread through the model domain (marked as green points in Figure 6). These four points are: Llangennith, on the Gower Peninsula, a popular surfing location; Scarweather Sands, the location of the calibration wave buoy and in the centre of the domain, thus providing an overall indication of change; a point offshore along the Vale of Glamorgan coast; and a point near the North Somerset coast, west of Weston-Super Mare, where population centres close to the coast mean coastal defence is important. No points were included further west along the North Devon coast since the large hard rock cliffs are unlikely to be affected by changes to wave conditions.

3.1 Mean wave conditions over a spring tidal cycle

To determine the changes in the wave conditions, the percentage change in wave heights over one spring tidal cycle were used. These percentage changes were calculated following the equation below:

$$Pecentatage\ change\ over\ a\ tidal\ cycle = \left(\frac{\sum_{t=0}^{t=12.42hrs} H_{barrage(t)}}{\sum_{t=0}^{t=12.42hrs} H_{no\ barrage(t)}} - 1 \right) \times 100 \qquad (9)$$

The percentage change in wave height across the estuary is shown in Figure 10. Positive percentage change indicates increases in wave height are caused by barrage construction. It can be seen that in general changes are within ±5% of the natural case. On the North Somerset coast, between Minehead and Weston-Super-Mare, average wave heights increase by 10% of the pre-barrage mean conditions with isolated increases larger than that. There are also larger increases at Tenby and to the west of Bideford. There are very local predicted increases around the South Gower Coast to the West of Swansea, due to a reduction in the tidal race around the headlands that previously caused significant wave dissipation and blocking. The most obvious area of wave height decrease is between Swansea and Porthcawl. Although the sum of wave height over the tidal cycle in post-barrage scenario is higher in some points, the maximum significant wave height is not higher for the post-barrage scenario at these points.

In order to better understand the tidal variation of this change, the four locations shown in Figure 6 are considered. The time series of wave height and water level for these locations are plotted in Figure 11. Cases with and without the barrage are shown on the same panel for each point. For the natural, no barrage case, wave heights are greater on the incoming tides, with times of peak wave height varying between 2hrs after low tide to 1hr before high tide, depending on location. Wave heights reduce on the outgoing tide, reaching a minimum before low water. The modulation at Llangennith approaches a sinusoidal shape with the other locations being less uniform. For all cases the tidal modulation of wave height over the tidal cycle is reduced by barrage construction; there is a slight reduction in the peak wave height and an increase in wave heights on the outgoing tide compared to the natural case. This increase on the outgoing tide is visibly larger than the decrease on the incoming tide for all points apart from the point at Llangennith. The points at Scarweather and the Vale Coast show the most noticeable relative increases.

Variations in the wave period and direction were also considered. While modulation in the mean wave period and wave direction were observable (Figure 12), this was less noticeable than for wave height. For the wave period there was only a slight reduction in the mean wave period for the outgoing tide; the maximum reduction in the mean wave period was 0.5s and the mean change was 0.1s. There was little change in the wave direction; the mean difference at Scarweather Sands was 2.2º and the maximum difference 4.3º. Depth-induced refraction of wave rays towards a shore-normal direction meant that such small differences in direction could be considered negligible. Therefore, the following sections will only consider wave height.

3.1.1 The importance of current-induced modulation

Tests of mean wave conditions run over a spring tidal cycle without currents (i.e. water level variations only) highlighted the importance of currents to the tidal modulation of wave conditions. Figure 13 shows a time series of water levels, wave heights, periods and directions at Scarweather Sands with no currents and Figure 14 shows a comparison at Scarweather Sands for the case with and without currents. It can be seen that the tidal elevation variation alone provides approximately half of the magnitude of modulation in the wave height, as compared to the case where currents are also included. More importantly, the implementation of a barrage does not affect the shape of this modulation when currents

are not included. In both cases wave heights take a sinusoidal form, with lower wave heights at low tide due to increased dissipation through bottom friction. Likewise, modulations of the mean wave period and wave direction follow sinusoidal shapes (Figure 13), with very little difference between the cases with and without a barrage. Therefore, it can be said that changes to the current fields, rather than changes to the water levels, most affect wave conditions in the Severn Estuary.

3.2 Modulation of wave height over a neap tide

Changes induced by a barrage over a neap tide including currents (with all of the following simulations including currents) display similar patterns to changes over a spring tide (Figure 15). There is a reduced relative increase at the east of the region of interest but a greater relative increase to the western half of the domain. There are larger relative increases in Bideford Bay and Tenby. The time series of changes for the four points (Figure 16) show some differences, both for the natural condition and the post-barrage condition. The magnitude of modulation of the natural condition is about half of the spring tide modulation. The point at Llangennith is similar to the spring tide case, apart from the reduced magnitude. The natural condition at Scarweather Sands is similar in shape, although the wave heights are marginally higher. With a barrage implemented, the modulation doubles in frequency, with a maxima occurring around mid-tide on both stages of the tide and a minima occurring shortly after high and low water. For the third point, offshore of the Vale coast, the peak is sharper with a faster reduction in the wave height. As for the case of the spring tide, the inclusion of a barrage reduces the reduction in the wave height for most of the outgoing tide, although the minima are of a similar height. The final point, i.e. west of Weston-Super-Mare, had showed similar findings to the case for a spring tide.

3.3 Swell Condition

Swell conditions were run over a spring tidal cycle. Figure 17 shows the percentage change in the cumulative wave height and Figure 18 shows the time series of the wave height and water level at the four sites considered in this analysis. There are less net changes for the swell condition over a spring tidal cycle than for previous tests; however, the same increases in the wave height around Weston-Super-Mare remain. Differences in the modulation over the tidal cycle between the barrage and natural cases are also less, although modulation is still reduced. In particular, wave heights prior to low tide are increased for the case with a barrage included.

3.4 Storm conditions

Under storm conditions, the relative changes are less than for the spring tide test with mean conditions when summed over a tidal cycle (Figure 19). Consideration of changes over a tidal cycle (Figure 20) showed that the pattern of tidal modulation was similar to the spring tide test with mean conditions.

4. Discussion

This study has used the third generation wave model Swan, forced with hydrodynamic conditions provided by the unstructured grid version of the DIVAST model, to model the changes in the wave conditions caused by the implementation of a Severn Barrage. The version of Swan used in this study has been modified to better cater for wave- current interactions. Validation of the model suggested that the model was over estimating the tidal modulation of wave heights. This may be due to the lack of wind input in the model simulations. Some qualification must be given to the results due to the proximity of the open boundary to the area of interest, however use of input data from the pre-existing hydro-dynamic model domain meant extending the model was unfeasible. In some areas there are large wave heights very close to shore, with this being likely to be caused by insufficiently detailed model grid resolution and bathymetric resolution, rather than actual regions of extreme wave focussing. In this study the barrage was represented to be wave absorbing: in reality, a certain amount of wave reflection will take place which will alter results in close proximity to the barrage. Close to the barrage wave heights are likely to increase due to reflections, with the magnitude dependant on the reflection co-efficient of the barrage design.

Tests described the natural tidal modulation in wave heights in the outer estuary; in general wave heights were at a minimum just before low tide and increased to a maximum at an hour or two before high tide, before reducing on the outgoing tide. Barrage construction reduced currents in the region which meant that the wave dissipation on the opposing current was less and the reduction on the ebb tide was less. In some cases, there was also a reduction in the maximum wave height at the peak. Net changes were calculated over one tidal cycle. In general changes were small, with average post barrage wave heights being within 5% of the natural wave heights. This suggests that barrage construction will have little impact on wave conditions over longer periods of time, despite there being changes in the intra-tidal detail of modulation; a good result for proponents of the Severn Barrage.

One consideration that may need further investigation is whether the impact of the increase in waves on the ebb tide will alter or affect sediment transport pathways in the nearshore. In much of the outer estuary there are strong longshore tidal currents, directed eastward on the incoming tide and westward on the outgoing tide. Previous sediment transport analysis has shown that net pathways are eastward in the nearshore zone and westward in the channel centre [56, 57]. Increased wave-induced mobilisation of sediment on the outgoing tide may increase westward transport in the nearshore and reduce the net eastward sediment transport pathways. Without a coupled wave-tide-sediment modelling study of the area, it is difficult to predict with any confidence the impact this may have on coastal erosion or accretion. However, much of the coastline is bounded by erosion resistant cliff or promontories which will reduce the potential for erosion. The exception to this is the dune backed coastline between Porthcawl and Swansea and the coastline around Weston-Super-Mare (coastally protected). Since these areas are sediment rich, it is postulated that while sediment transport pathways may change slightly, increases in erosion are unlikely.

There are some areas that show a larger increase in wave heights over a tidal cycle, most notably along the North Somerset coast between Minehead and Weston-Super-Mare where wave heights post construction approach 20% above the natural condition. However, the shallow, gently sloping seabed in the region means that waves undergo depth limited breaking some distance from the shoreline and so any increased wave height should have

no effect on coastal erosion or flooding in the region. Moreover, the maximum wave height does not occur at the same time as high water, which makes the waves less significant in terms of flooding.

Swell conditions were tested primarily to determine any likely impact on recreational surfing. Barrage implementation had less impact on swell conditions than on mean wave conditions; however, it still led to an increase in the wave heights on the outgoing tide. Anecdotal evidence suggests that, in this region, surfers only participate in their sport on the incoming tide when wave heights are larger. Given that barrage implementation is predicted to increase wave heights on the outgoing tide under all conditions tested, then it could be argued that barrage construction may actually increase the time suitable for surfing. In order to confirm this prediction with more certainty, higher resolution bathymetric data would be needed along the coast to be able to model breaking wave heights more accurately along the beaches.

Storm conditions were tested given the potential for large morphological change and loss of assets under such conditions. Importantly, maximum wave heights did not show large increases after barrage construction. For the sites at Llangennith and Scarweather Sands maximum wave heights actually decreased marginally. Net changes showed the same patterns as for other tests, with increases along the North Somerset coast. This increase represents increased duration of large waves, rather than waves that are larger than the natural case. However, it would be prudent for any environmental impact assessment studies for a barrage to assess storm impacts in this area.

5. Conclusions

Construction of a Severn Barrage would affect both water levels and currents in the Severn Estuary and Bristol Channel. Currents are more significant than water levels in modulating short period wave heights. Changes to currents and water levels by a barrage construction would affect the already present tidally-induced modulation of wave conditions in the estuary. However, these changes would largely be small; wave heights are between ±5% of the natural case for most areas. In areas where the effect is larger, heights are under 20% greater than the natural case. The shape of the modulation over the tidal cycle for natural conditions is largely similar for all tested points. There is a peak in the wave height on the incoming tide and a reduction in the heights on the outgoing tide, dropping to a minimum just before low tide. Barrage implementation changes this modulation, primarily leading to an increase in the wave heights on the outgoing tide. The area where an increase in the wave height is most noticeable is along the North Somerset coast, between Weston-Super-Mare and Minehead. There are also predicted to be increases in some areas around the south coast of the Vale of Glamorgan. Predicted increases in wave heights are not co-incident with high water and therefore these changes are unlikely to pose increased flood risk. The most prominent area of net decrease along the coast is at Port Talbot, to the east of Swansea.

6. Acknowledgments

This research has been carried out as part of both the LCRI and MAREN projects, which are part funded by the Welsh Government, the Higher Education Funding Council for Wales, the Welsh European Funding Office, and the European Regional Development Fund (ERDF) Convergence and Atlantic Area Transnational (INTERREG IV) Programmes. The authors wish to acknowledge their financial support.

The authors acknowledge the use of Battri and Triangle in mesh generation. Andreas van der Westhuysen is thanked for providing his modified Swan source code which allowed us to use his improvements that better cater for wave-current interaction. The authors would like to thank the two anonymous reviewers' for their detailed reading of the manuscript and constructive criticism.

References

[1] S. P. Neill, J. R. Jordan, and S. J. Couch, "Impact of tidal energy converter (TEC) arrays on the dynamics of headland sand banks," *Renewable Energy,* vol. 37, pp. 387-397, 2012.

[2] S. P. Neill, E. J. Litt, S. J. Couch, and A. G. Davies, "The impact of tidal stream turbines on large-scale sediment dynamics," *Renewable Energy,* vol. 34, pp. 2803-2812, 2009.

[3] R. H. Charlier, "Forty candles for the Rance River TPP tides provide renewable and sustainable power generation," *Renewable & Sustainable Energy Reviews,* vol. 11, pp. 2032-2057, 2007.

[4] N. S. Power, "Annapolis tidal power plant," 2009. Available online: www.power.about.com/gi/dynamic/offsite.htm

[5] F. O. Rourke, F. Boyle, and A. Reynolds, "Tidal energy update 2009," *Applied Energy,* vol. 87, pp. 398-409, 2010

[6] I. Fairley, P. Evans, C. Wooldridge, M. Willis, and I. Masters, "Evaluation of tidal stream resource in a potential array area via direct measurements," *Renewable Energy,* vol. 57, pp. 70-78, 2013.

[7] DECC, "Severn Power Tidal Power Feasibility Study Conclusions and Summary Report," 2010.

[8] Department of Energy, "Central electricity generating board and Severn tidal power group, the Severn Barrage project: general report," London1989.

[9] R. McGlynn and E. Inst Civil, Regional economic-impact of the Severn Barrage. London: Thomas Telford Services Ltd, 1990.

[10] R. Ahmadian, R. Falconer, and B. Lin, "Hydro-environmental modelling of proposed Severn barrage, UK," *P I Civil Eng.- Energ,* vol. 163, pp. 107-117, 2010.

[11] R. Ahmadian , A. I. Olbert, M. Hartnett, and R. A. Falconer, "Impacts of Sea Level Rise on the Severn Estuary and the Proposed Severn Barrage," *Estuaries and Coasts,* (in press), 2014.

[12] C. Frid, E. Andonegi, J. Depestele, A. Judd, D. Rihan, S. I. Rogers, and E. Kenchington, "The environmental interactions of tidal and wave energy generation devices," *Environmental Impact Assessment Review,* vol. 32, pp. 133-139, Jan.

[13] J. Xia, R. A. Falconer, and B. Lin, "Impact of different operating modes for a Severn Barrage on the tidal power and flood inundation in the Severn Estuary, UK," *Applied Energy,* vol. 87, pp. 2374-2391, 2010

[14] J. Q. Xia, R. A. Falconer, and B. L. Lin, "Hydrodynamic impact of a tidal barrage in the Severn Estuary, UK," *Renewable Energy,* vol. 35, pp. 1455-1468, 2010

[15] M. Kadiri, R. Ahmadian, B. Bockelmann-Evans, W. Rauen, and R. Falconer, "A review of the potential water quality impacts of tidal renewable energy systems," *Renewable & Sustainable Energy Reviews,* vol. 16, pp. 329-341, 2012

[16] N. H. K. Burton, A. J. Musgrove, M. M. Rehfisch, and N. A. Clark, "Birds of the Severn Estuary and Bristol Channel: Their current status and key environmental issues," *Marine Pollution Bulletin,* vol. 61, pp. 115-123. 2010

[17] J. Osment, P. Halstead, N. Pontee, B. Hamer, and R. Harvey, "Reassessing the Severn Barrage: Operational Modes and their Impacts " in *ICE Coastal Management* Belfast, 2011.

[18] M. W. Aprahamian, C. D. Aprahamian, and A. M. Knights, "Climate change and the green energy paradox: the consequences for twaite shad Alosa fallax from the River Severn, U.K," *Journal of Fish Biology,* vol. 77, pp. 1912-1930, Nov 2010.

[19] M. Willis, I. Masters, S. Thomas, R. Gallie, J. Loman, A. Cook, R. Ahmadian , R. Falconer, B. Lin, G. H. Gao, M. Cross, T. N. Croft, A. T. Williams, M. Muhasilovic, I. Horsfall, R. Fidler, C. Wooldridge, I. Fryett, P. Evans, T. O'Doherty, D. O'Doherty, and A. Mason-Jones, "Tidal turbine deployment in the Bristol Channel: a case study," *Proceedings of the Institution of Civil Engineers - Energy,* vol. 163, pp. 93–105, 2010.

[20] J. S. Pethick, R. K. A. Morris, and D. H. Evans, "Nature conservation implications of a Severn tidal barrage - A preliminary assessment of geomorphological change," *Journal for Nature Conservation,* vol. 17, pp. 183-198, 2009.

[21] R. Kirby, "Distribution, transport and exchanges of fine sediment, with tidal power implications: Severn Estuary, UK," *Marine Pollution Bulletin,* vol. 61, pp. 21-36, 2010.

[22] G. J. C. Underwood, "Microphytobenthos and phytoplankton in the Severn estuary, UK: Present situation and possible consequences of a tidal energy barrage," *Marine Pollution Bulletin,* vol. 61, pp. 83-91, 2010

[23] J. Wolf and D. Prandle, "Some observations of wave-current interaction," *Coastal Engineering,* vol. 37, pp. 471-485,1999.

[24] R. Ahmadian, R. Falconer, and B. Bockelmann-Evans, "Far-field modelling of the hydro-environmental impact of tidal stream turbines," *Renewable Energy,* vol. 38, pp. 107-116, 2012.

[25] R. Ahmadian and R. A. Falconer, "Assessment of array shape of tidal stream turbines on hydro-environmental impacts and power output," *Renewable Energy,* vol. 44, pp. 318-327, 2012.

[26] J. Xia, R. A. Falconer, and B. Lin, "Impact of different tidal renewable energy projects on the hydrodynamic processes in the Severn Estuary, UK," *Ocean Modelling,* vol. 32, pp. 86-104, 2010.

[27] J. R. Bidlot and M. W. Holt, "Numerical wave modelling at operational weather centres," *Coastal Engineering,* vol. 37, pp. 409-429, 1999.

[28] J. Xia, R. A. Falconer, and B. Lin, "Numerical model assessment of tidal stream energy resources in the Severn Estuary, UK," *Proceedings of the Institution of Mechanical Engineers Part a-Journal of Power and Energy,* vol. 224, pp. 969-983, 2010

[29] R. A. Falconer, J. Q. Xia, B. L. Lin, and R. Ahmadian, "The Severn Barrage and other tidal energy options: Hydrodynamic and power output modelling," *Science in China Series E-Technological Sciences,* vol. 52, pp. 3413-3424, 2009.

[30] G. P. Evans, B. M. Mollowney, and N. C. Spoel, "Two-dimensional Modelling of the Bristol Channel, UK.," in *Proceedings of the conference on estuarine and coastal modeling* pp 331-340, 1990

[31] R. J. Uncles, "A Numerical-Simulation of the Vertical and Horizontal M2 Tide in the Bristol Channel and Comparisons with Observed Data," *Limnology and Oceanography,* vol. 26, pp. 571-577, 1981

[32] J. Xia, R. A. Falconer, B. Lin, and G. Tan, "Estimation of annual energy output from a tidal barrage using two different methods," *Applied Energy,* vol. 93, pp. 327-336, 2012

[33] B. F. Sanders, "Non-reflecting boundary flux function for finite volume shallow-water models," *Advances in Water Resources,* vol. 25, pp. 195-202, 2002.
[34] N. Booij, R. C. Ris, and L. H. Holthuijsen, "A third-generation wave model for coastal regions - 1. Model description and validation," *Journal of Geophysical Research-Oceans,* vol. 104, pp. 7649-7666, 1999.
[35] M. Zijlema, "Computation of wind-wave spectra in coastal waters with SWAN on unstructured grids," *Coastal Engineering,* vol. 57, pp. 267-277, 2010.
[36] R. C. Ris, L. H. Holthuijsen, and N. Booij, "A third-generation wave model for coastal regions - 2. Verification," *Journal of Geophysical Research-Oceans,* vol. 104, pp. 7667-7681, 1999.
[37] G. Iglesias and R. Carballo, "Offshore and inshore wave energy assessment: Asturias (N Spain)," *Energy,* vol. 35, pp. 1964-1972, 2010.
[38] G. Iglesias, M. Lopez, R. Carballo, A. Castro, J. A. Fraguela, and P. Frigaard, "Wave energy potential in Galicia (NW Spain)," *Renewable Energy,* vol. 34, pp. 2323-2333, 2009.
[39] L. Rusu and C. G. Soares, "Wave energy assessments in the Azores islands," *Renewable Energy,* vol. 45, pp. 183-196, 2012.
[40] H. C. M. Smith, C. Pearce, and D. L. Millar, "Further analysis of change in nearshore wave climate due to an offshore wave farm: An enhanced case study for the Wave Hub site," *Renewable Energy,* vol. 40, pp. 51-64, Apr 2012.
[41] A. J. van der Westhuysen, "Improved modelling of wave-current interaction in Swan," in *Coastal Engineering 2010* Hamburg: ASCE, 2010.
[42] R. C. Ris and L. H. Holthuijsen, "Spectral modelling of current-induced wave blocking," in *25th International Conference on Coastal Engineering* Orlando, Florida: ASCE, 1996, pp. 1247-1254. 1996
[43] A. J. van der Westhuysen, "Spectral modeling of wave dissipation on negative current gradients," *Coastal Engineering,* vol. 68, pp. 17-30, Oct 2012.
[44] K. Hasselman, "On the spectral dissipation of ocean waves due to whitecapping," *Boundary - Layer Meteorology,* vol. 6, pp. 107-127, 1974.
[45] G. J. Komen, S. Hasselmann, and K. Hasselman, "On the existance of a developed wind-sea spectrum," *Journal of Physical Oceanography,* vol. 14, pp. 1271-1285, 1984.
[46] J. A. Battjes and J. P. F. M. Janssen, "Energy Loss and set up due to breaking of random waves," in *16th International Conference Coastal Engineering*: ASCE, pp. 569-587. 1978
[47] A. Chawla and J. T. Kirby, "Monochromatic and random wave breaking at blocking points," *Journal of Geophysical Research,* vol. 107, 2002.
[48] A. J. van der Westhuysen, M. Zijlema, and J. A. Battjes, "Nonlinear saturation-based whitecapping dissipation in SWAN for deep and shallow water," *Coastal Engineering,* vol. 54, pp. 151-170, 2007.
[49] J. Alves and M. L. Banner, "Performance of a saturation-based dissipation-rate source term in modeling the fetch-limited evolution of wind waves," *Journal of Physical Oceanography,* vol. 33, pp. 1274-1298, 2003.
[50] L. Yan, "An improved wind input source term for third generation ocean wave modelling," Royal Dutch Meteorological Institute, 1987.
[51] R. J. Lai, S. R. Long, and N. E. Huang, "Laboratory studies of wave-current interaction – kinematics of the strong interaction," *Journal of Geophysical Research-Oceans,* vol. 94, pp. 16201-16214, 1989.
[52] I. K. Suastika, M. P. C. de Jong, and J. A. Battjes, "Experimental study of wave blocking," in *Castal Engineering 2000*: ASCE, pp. 227-240. 2000.
[53] Swan 40.81 User Manual, Delft Technical University. 2006
[54] A. Bilgili, K. W. Smith, and D. R. Lynch, "BatTri: A two-dimensional bathymetry-based unstructured triangular grid generator for finite element circulation modeling," *Computers & Geosciences,* vol. 32, pp. 632-642, 2006.

[55] J. S. Shewchuk, "Triangle: Engineering a 2D Quality Mesh Generator and Delauney Triangulator," in *Lecture Notes in Computer Science*. vol. 1148 Berlin: Springer-Verlag, pp. 203-222, 1996

[56] M. B. Collins, "Sediment fluxes in the Bristol Channel," in *Annual Conference of the Ussher Society*, 1989.

[57] P. T. Harris and M. B. Collins, "Sand transport in the Bristol Channel - bedload parting zone or mutually evasive transport pathways," *Marine Geology,* vol. 101, pp. 209-216, 1991.

List of figures

Figure 1: Map of Severn Estuary and Bristol Channel. The sub-map shows the location of the Severn Estuary in the wider UK. Marked on the map is the barrage location, the two model boundaries and model calibration points. Also labelled are certain locations mentioned in the text.

Figure 2: Power spectral density plots for: (a) wave height, (b) peak wave period, (c) wave direction and (d) wave directional spread. The semi-diurnal tidal frequency is marked by a red line. This plot illustrates the observed tidal modulation of wave climate in the Bristol Channel

Figure 3: Plots of modelled and measured parameters, showing good agreement between predicted and measured; (a) current speed, and (b) current direction at 51^{o}14.2'N, 3^{o}21.1'W (B on Figure 1) and (c) water level at the NTSLF gauge at Mumbles (A on Figure 1). From [7]

Figure 4: A plot of the spring-neap cycle modelled with DIVAST, with the calibration period and the spring and neap test cases marked by grey bars.

Figure 5: Tidal current velocities for the natural (no barrage) case on the left and for the case with the barrage on the right. Arrows indicate non-scaled current direction and colour shading indicates velocity magnitudes. Only a sub-section of the domain is shown to allow higher resolution of the area of interest.

Figure 6: Computational mesh used in the model with the barrage marked in red, the location of the model output point used for the wave boundary conditions in blue and the four representative points used in the analysis in green.

Figure 7: Wave measurements (o) and model predictions (-) for a wave buoy at Scarweather Sands over the validation period (no barrage).

Figure 8: A normalised spectral density plot for the model output (black) and measured buoy data (grey) clearly showing the similarity in peak at the semi-diurnal frequency.

Figure 9: Representation of data used to determine wave boundary conditions. The vertical axis indicates percentage occurrence of a wave period – wave direction pair and colour shading shows mean wave height for that pair.

Figure 10: Percentage change to wave height over one spring tidal cycle.

Figure 11: Time series of wave height and water level for the four points over a spring tide. The pre barrage water level is marked in black and the pre-barrage wave height in blue. Wave heights for the barrage case are marked in red and water level in grey.

Figure 12: Modulation of: (a) wave period and (b) wave direction at Scarweather Sands. Pre-barrage water levels are marked in black and post barrage levels in grey. Pre barrage parameters are marked in blue and post barrage in red.

Figure 13: Time series of: (a) wave height; (b) wave period and (c) wave direction at Scarweather Sands with only water level variation. Pre-barrage water levels are marked in

black and post-barrage water levels in grey. Pre-barrage parameters are marked in blue and post-barrage parameters in red.

Figure 14: Comparison of wave heights with currents (red) and without currents (blue) at Scarweather Sands. The barrage case is shown for a solid line and no barrage with a dotted line.

Figure 15: Percentage change in cumulative wave height over a tidal cycle for a neap tide with mean conditions.

Figure 16: Time series of wave height and water level at the four sites over a neap tidal cycle. The pre barrage water level is marked in black and the pre-barrage wave height in blue. Wave heights for the barrage case are marked in red and the water level in grey.

Figure 17: percentage change in wave height summed over a spring tidal cycle for swell wave conditions.

Figure 18: Time series of wave height and water level at the four sites over a spring tidal cycle with swell wave conditions. The pre barrage water level is marked in black and the pre-barrage wave height in blue. Wave heights for the barrage case are marked in red and water level in grey.

Figure 19: A plot of percentage change in wave height summed over a tidal cycle for storm conditions.

Figure 20: Time series of wave height and water level at the four sites over a spring tidal cycle for storm wave conditions. The pre barrage water level is marked in black and the pre-barrage wave height in blue. Wave heights for the barrage case are marked in red and water level in grey.

List of Tables

Table 1: Hydrodynamic model parameters

Table 2: Summary of the different wave conditions used.

Model parameter	Value
Angle of latitude (Deg)	51.42
Maning's number	0.022
Minimum depth for flooding and drying (m)	0.10
Time step (s)	1.0
Maximum grid size (m^2)	373
Minimum grid size (m^2)	956,714
Domain size (km^2)	5,668

	H_s (m)	T_{m01} (s)	Direction (deg.)	D_{spr} (deg.)
Mean	1.6	5.6	89	17.5
Storm	5.7	9.25	92.5	17.5
Swell	1.8	13	87	17.5

Figure 1
Click here to download high resolution image

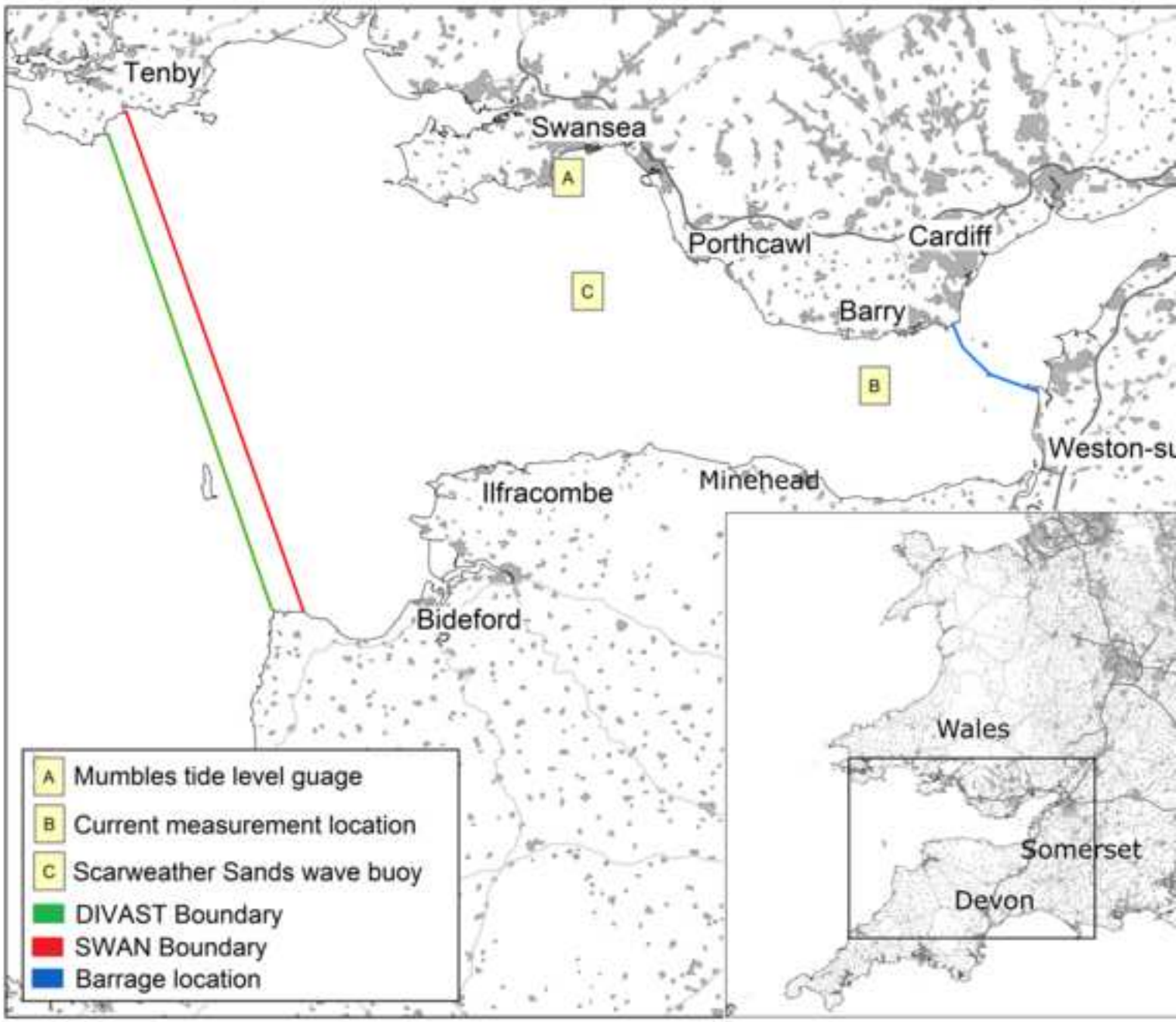

Figure 2
Click here to download high resolution image

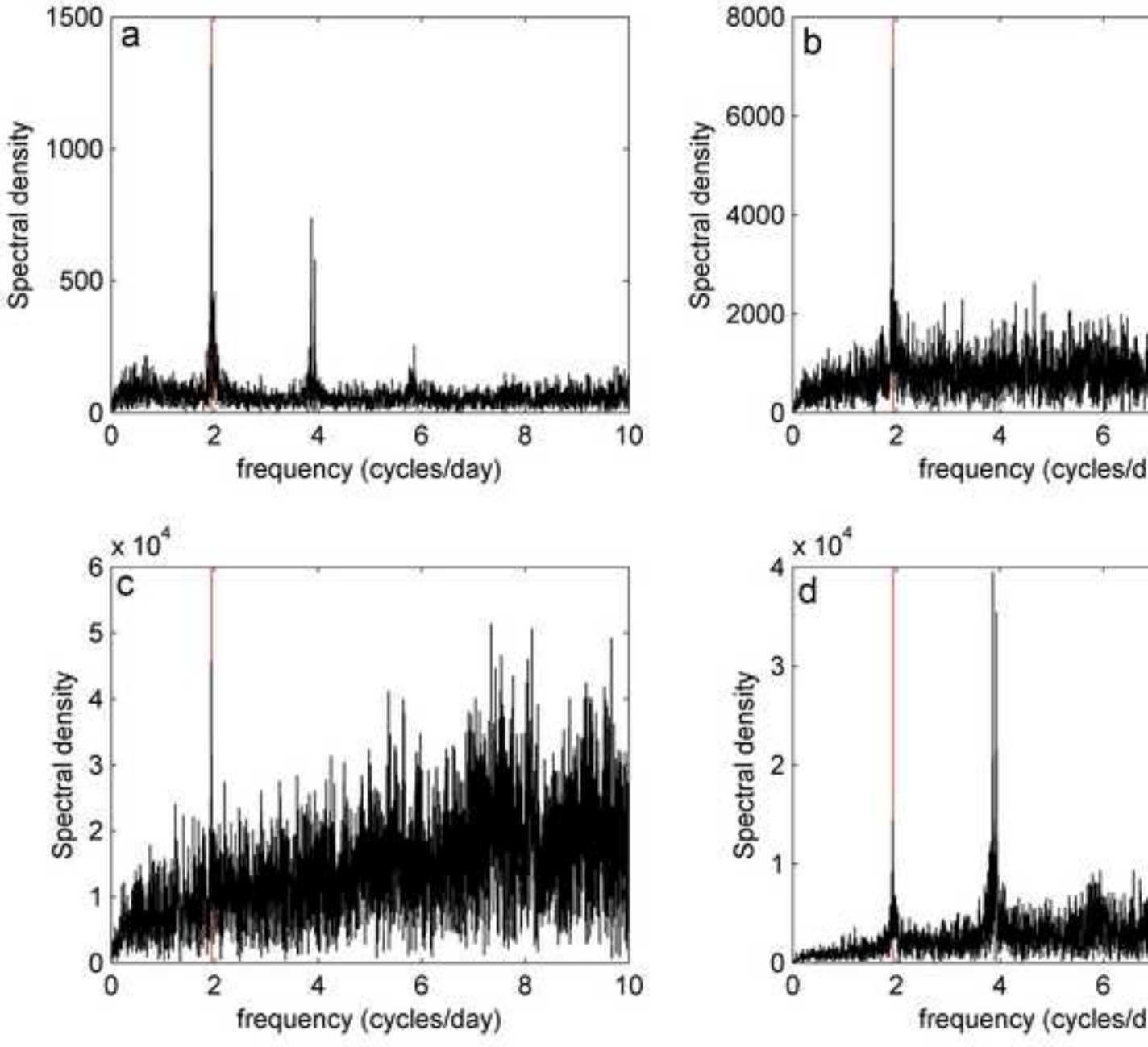

Figure 3
Click here to download high resolution image

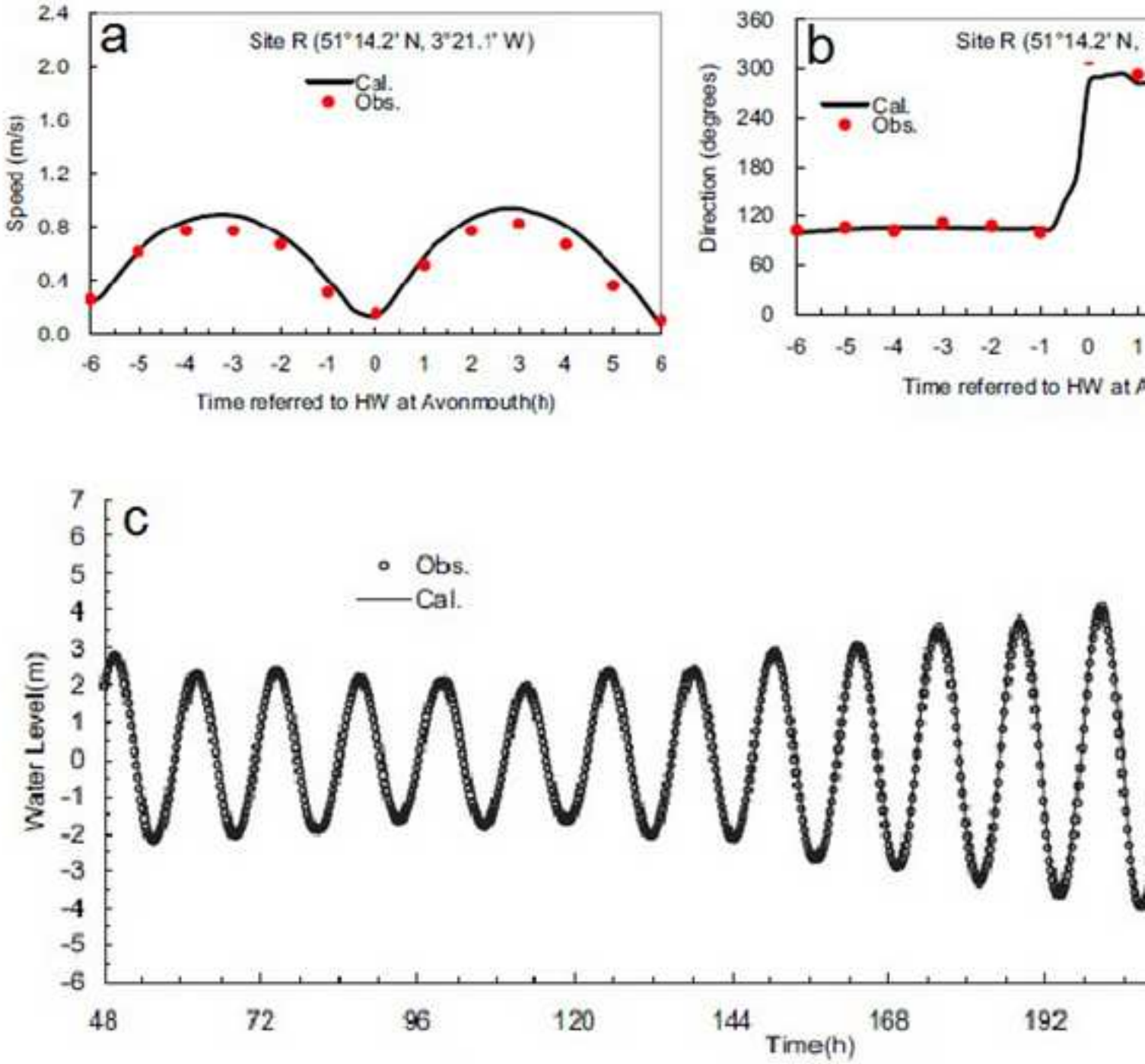

Figure 4
Click here to download high resolution image

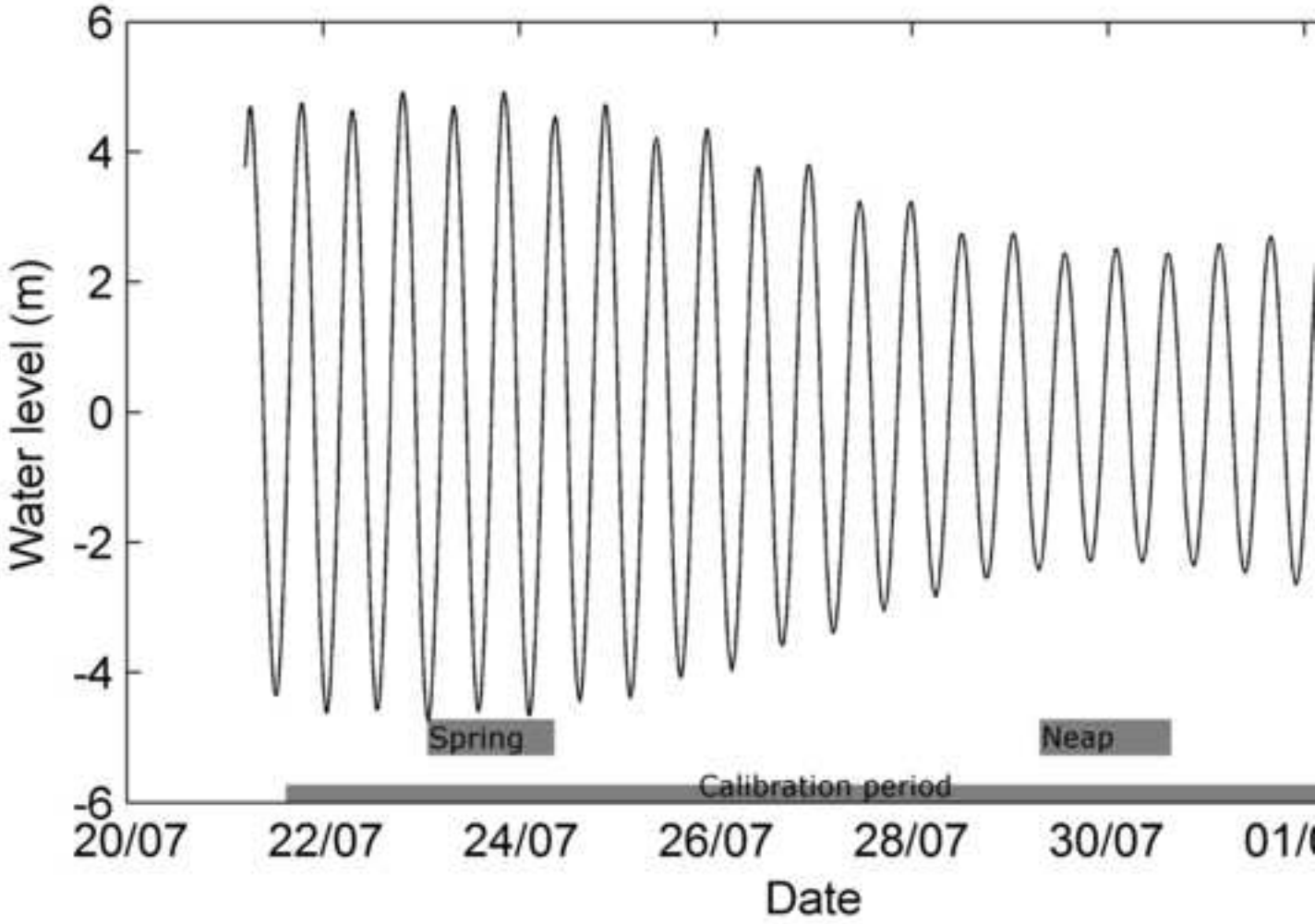

Figure 5

Click here to download high resolution image

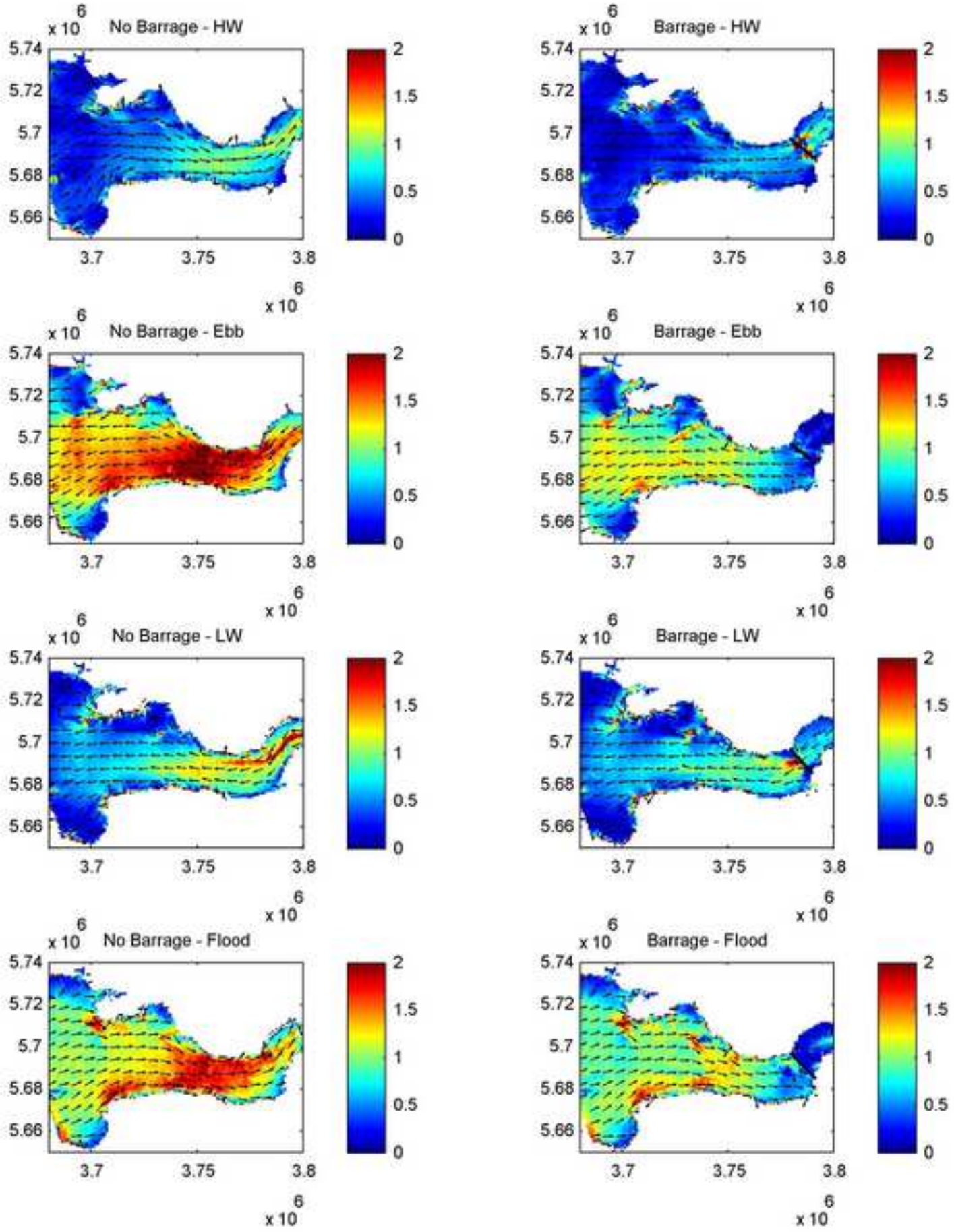

Figure 6
Click here to download high resolution image

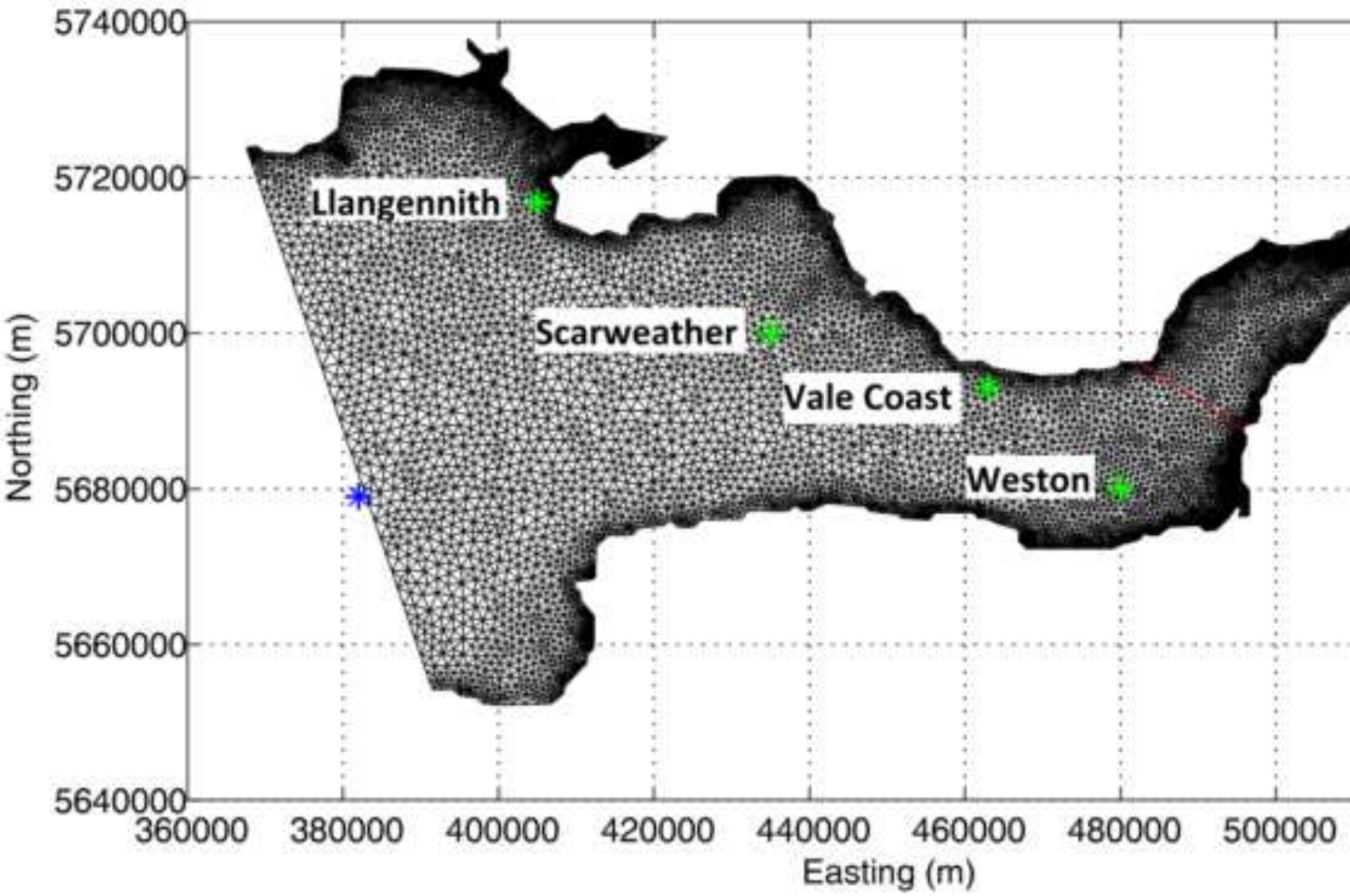

Figure 7
Click here to download high resolution image

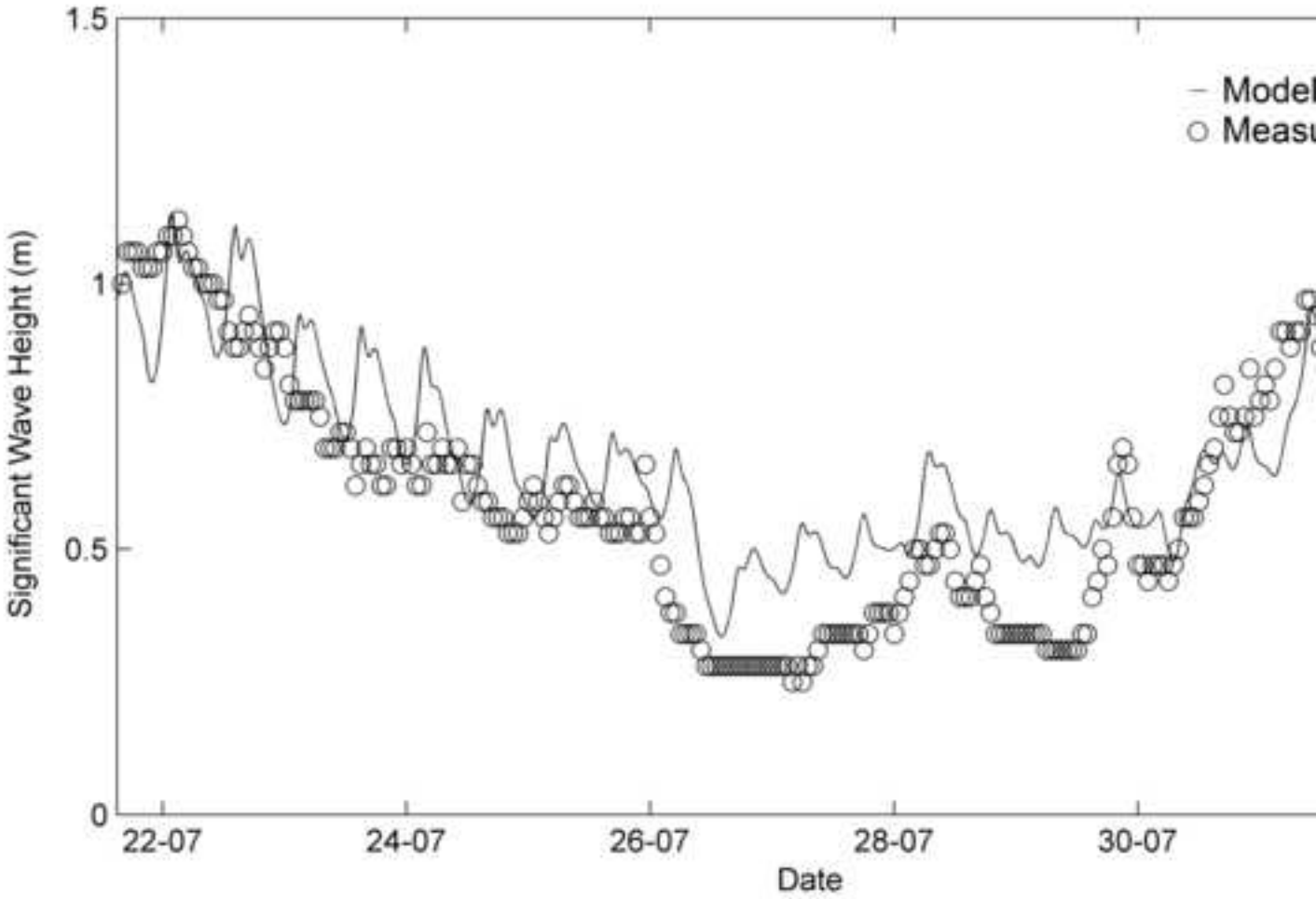

Figure 8
Click here to download high resolution image

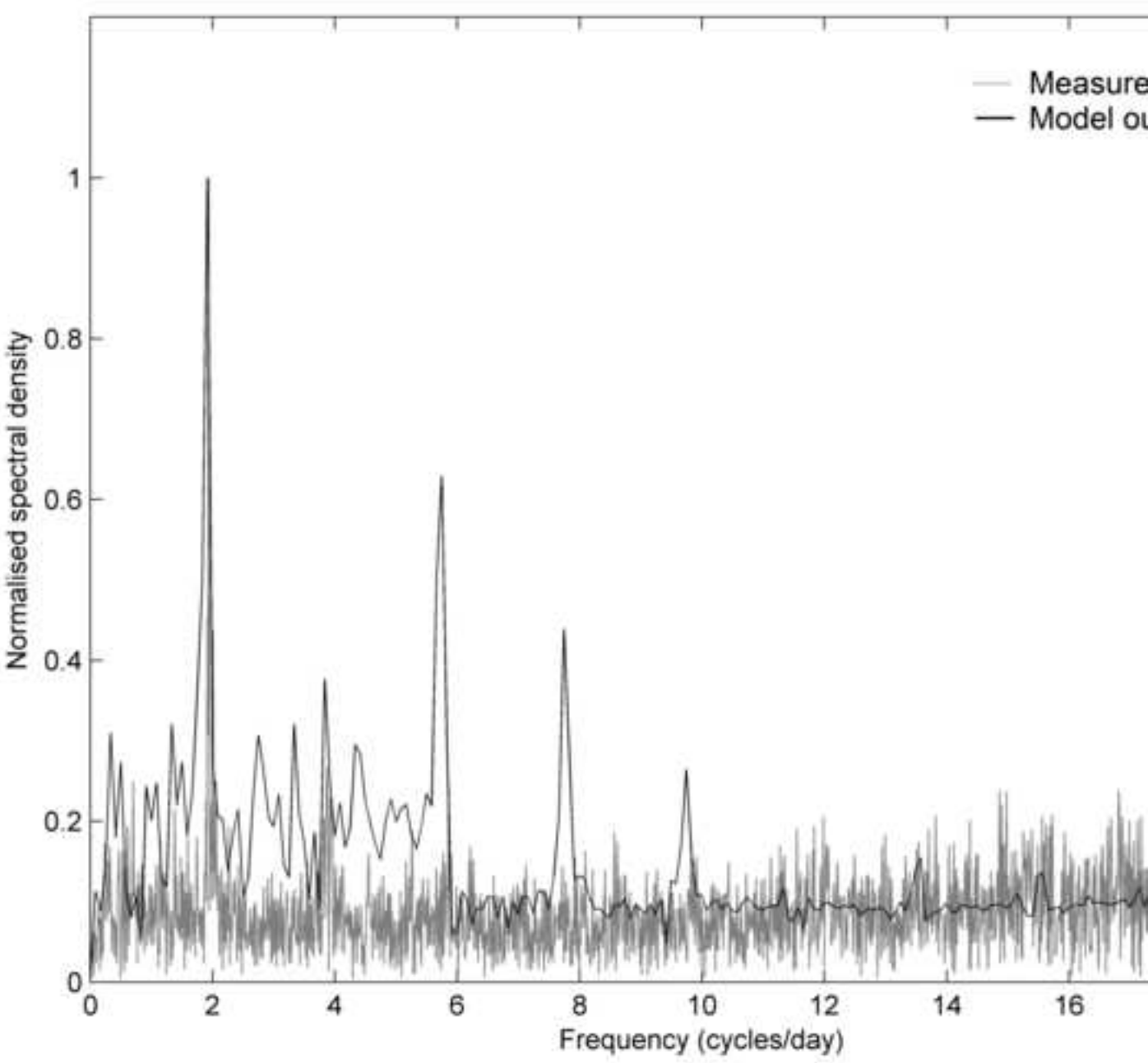

Figure 9
Click here to download high resolution image

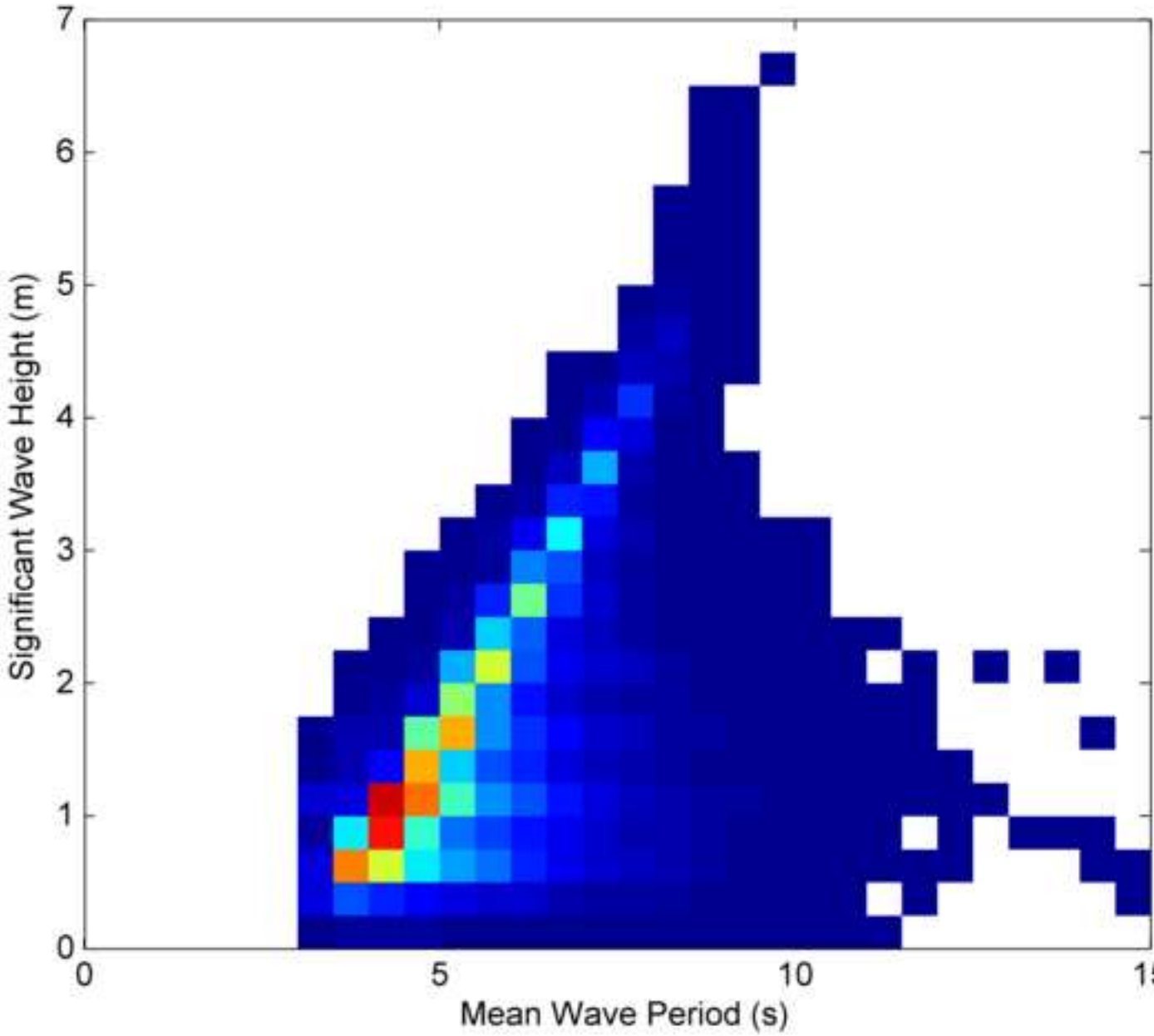

Figure 10
Click here to download high resolution image

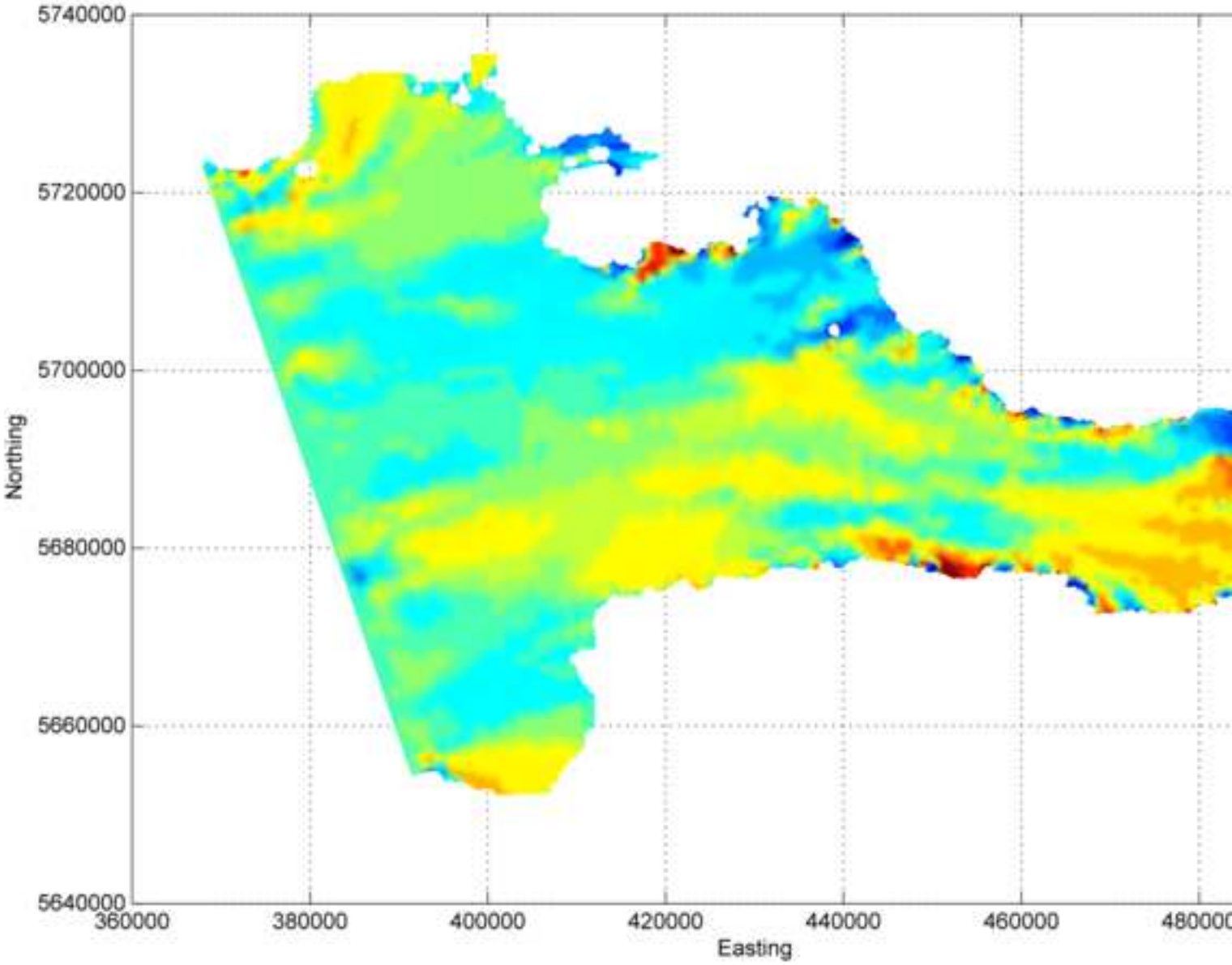

Figure 11
Click here to download high resolution image

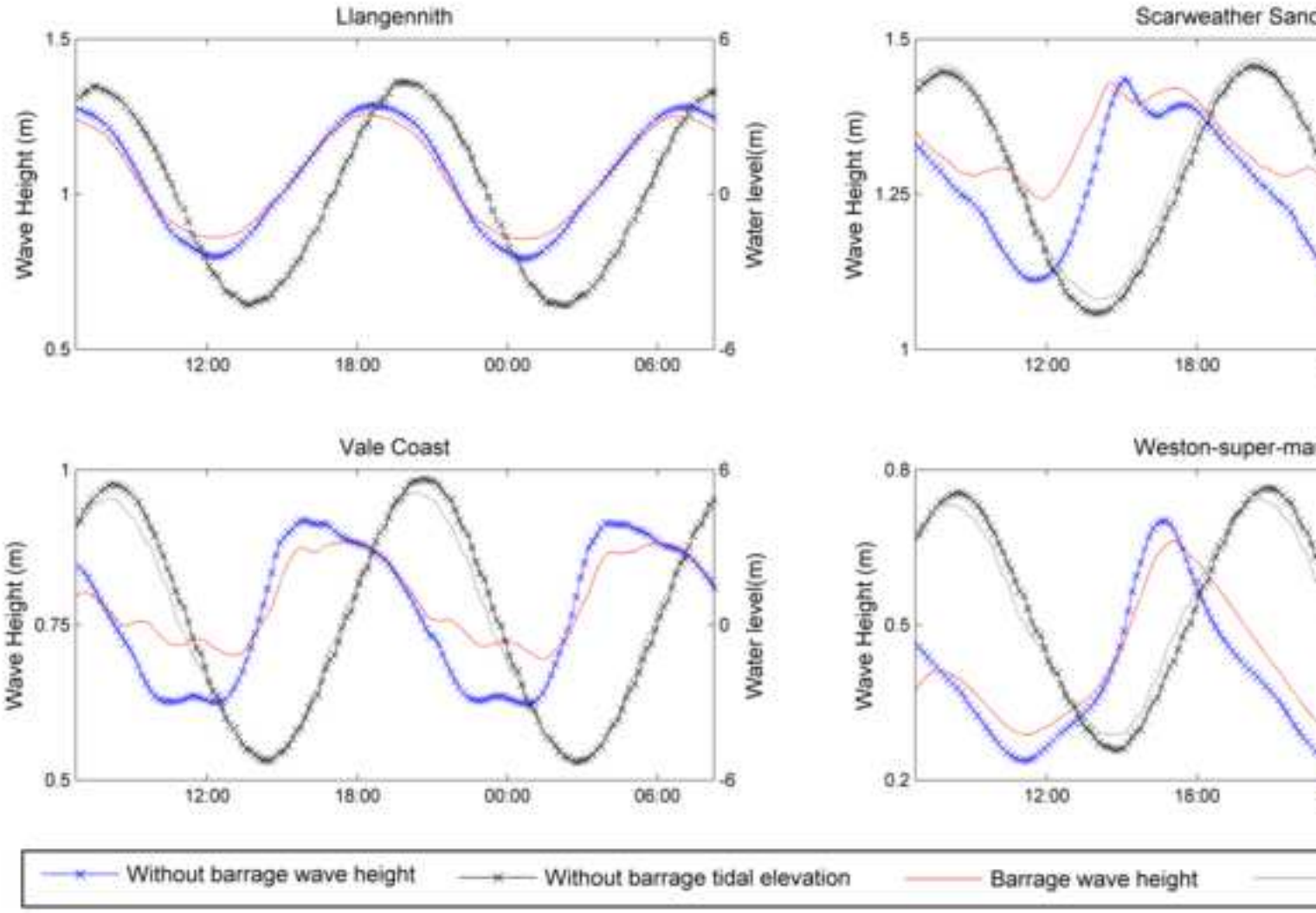

Figure 12
Click here to download high resolution image

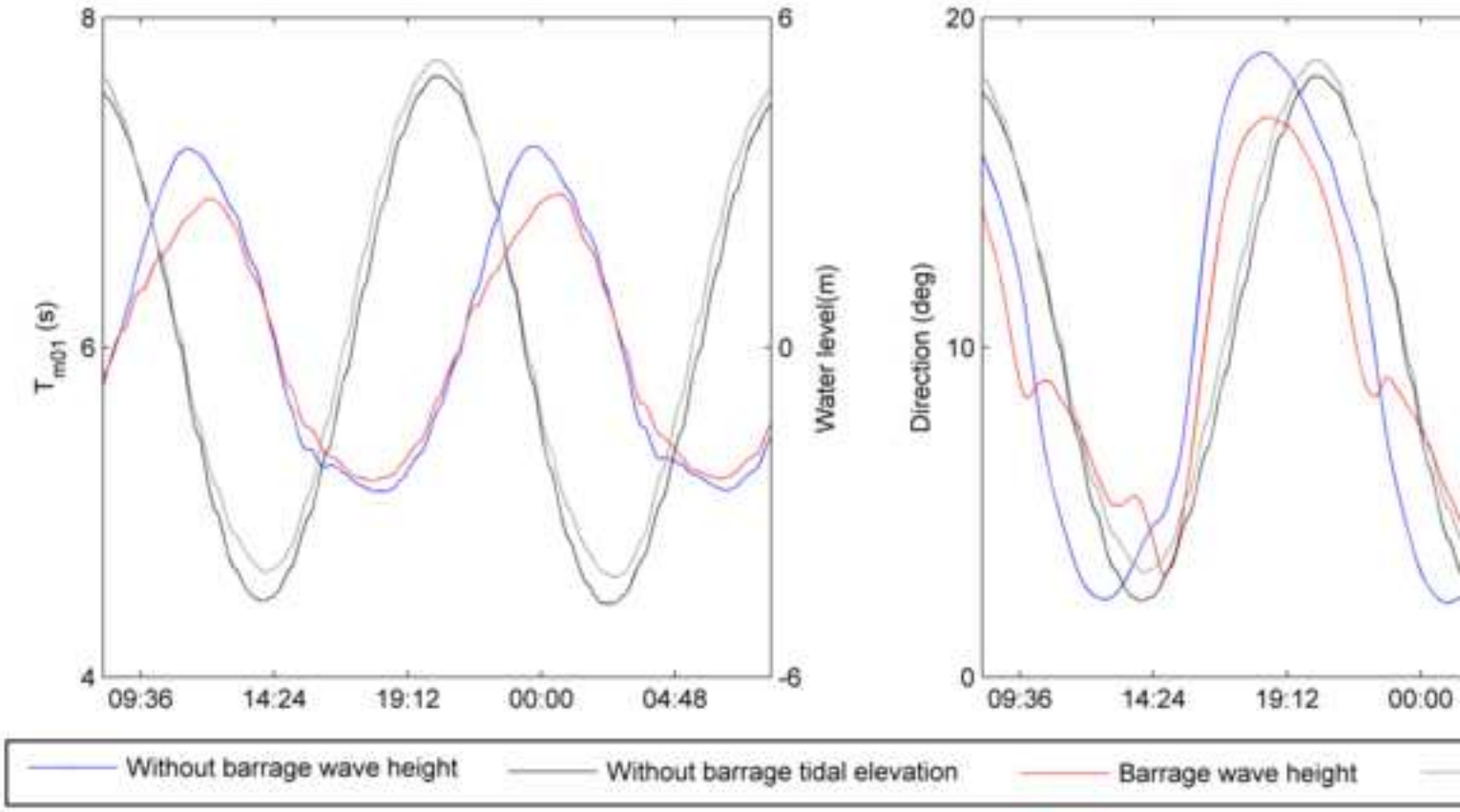

Figure 13

Click here to download high resolution image

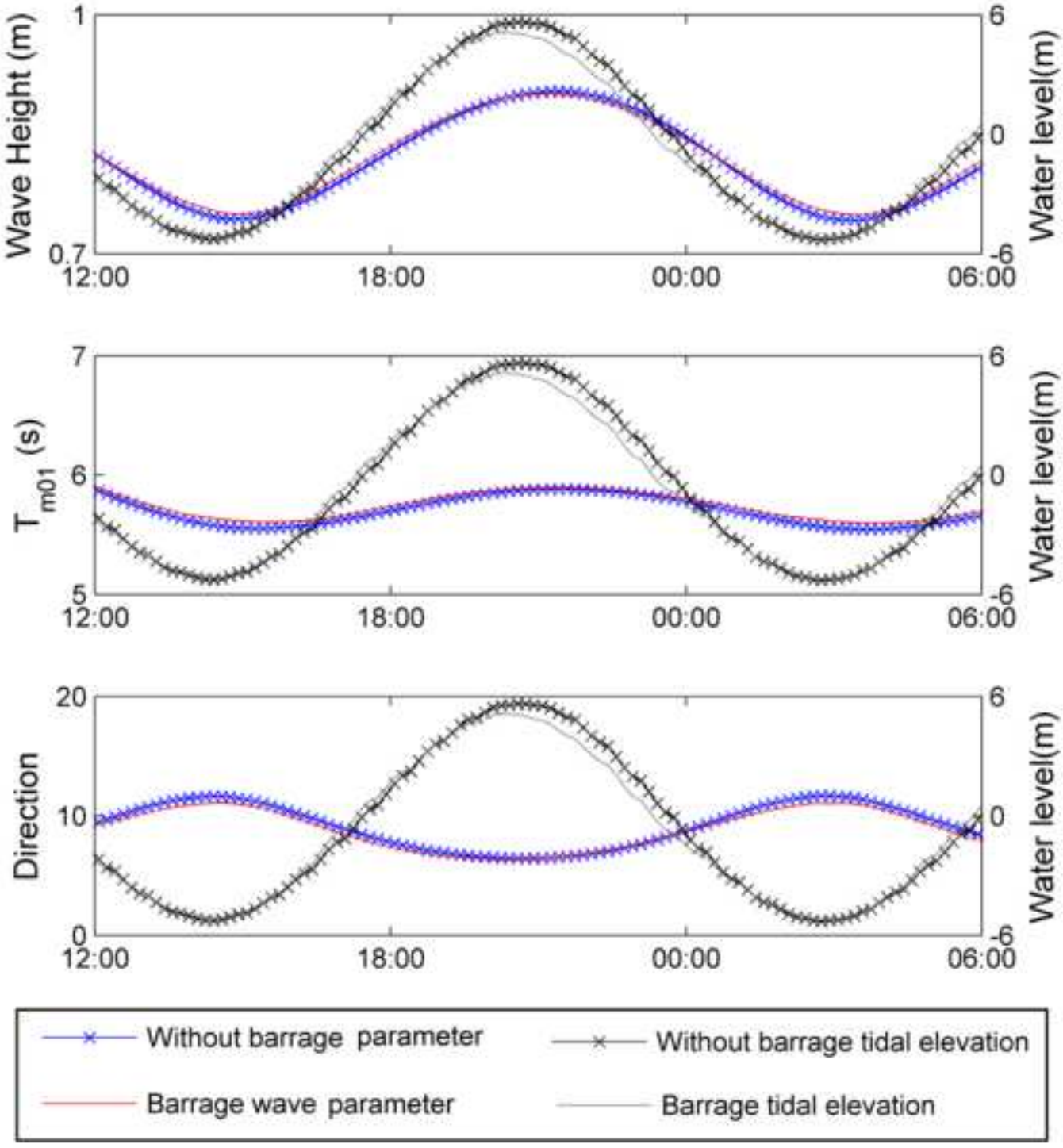

Figure 14
Click here to download high resolution image

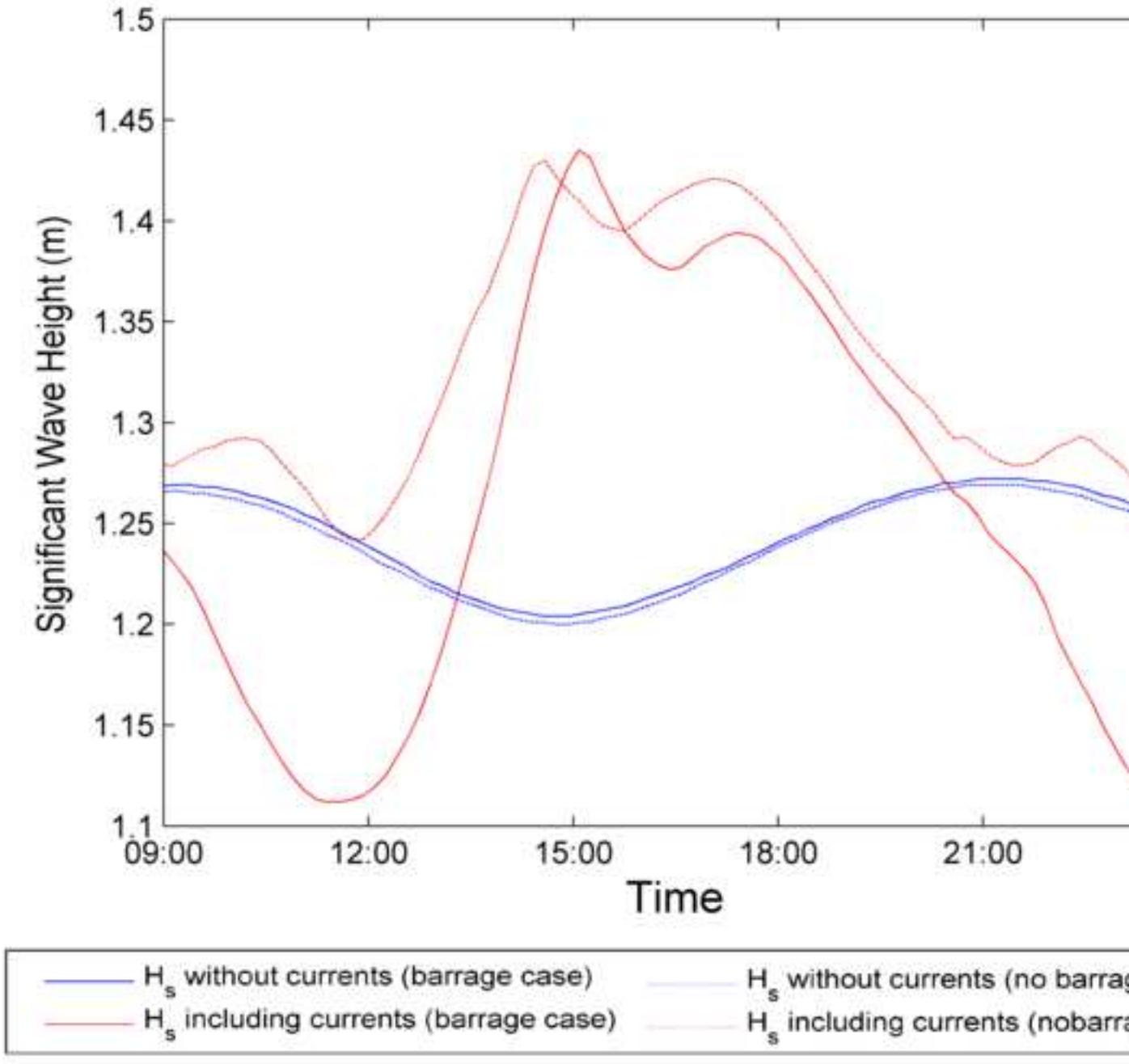

Figure 15
Click here to download high resolution image

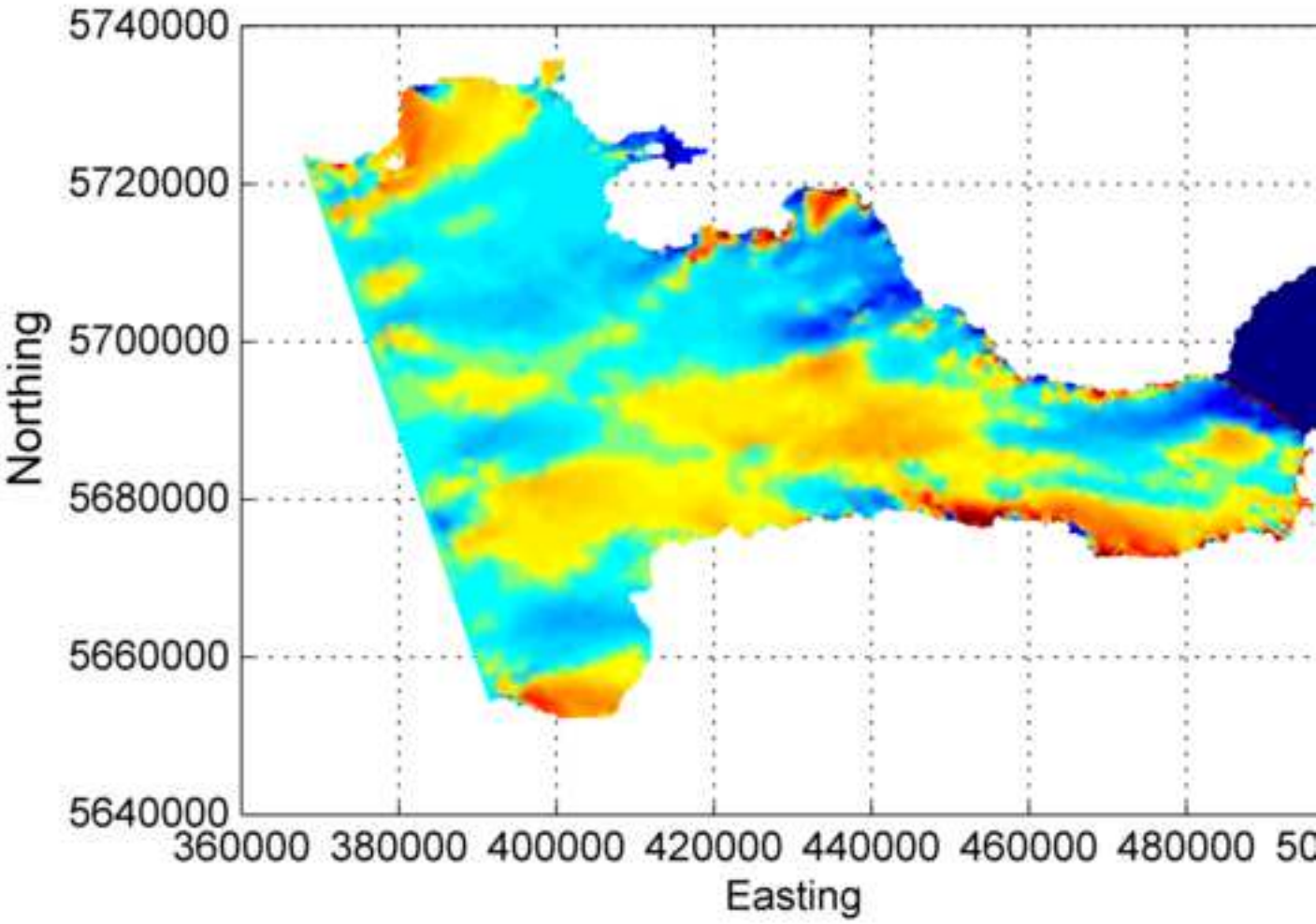

Figure 16
Click here to download high resolution image

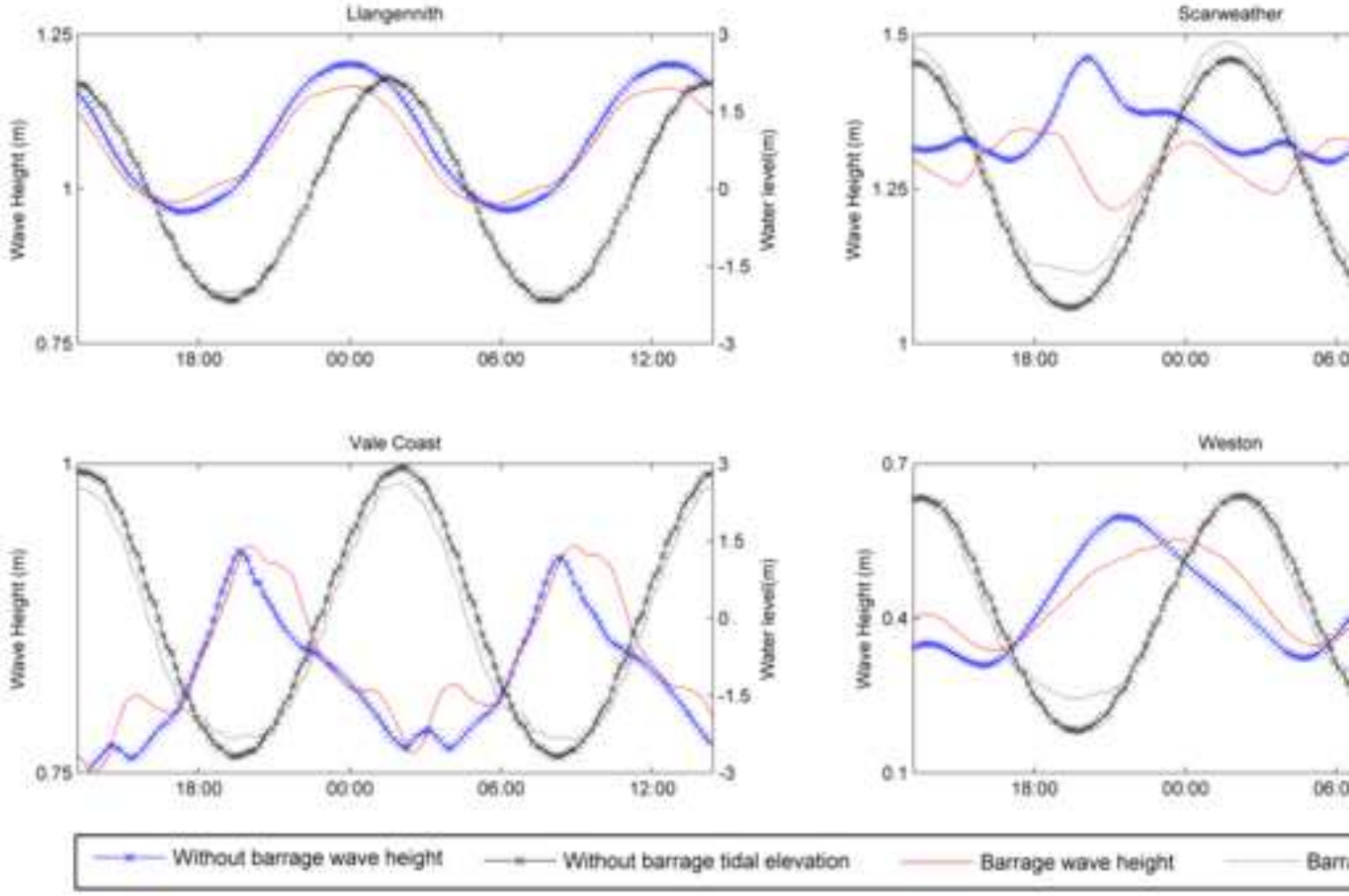

Figure 17
Click here to download high resolution image

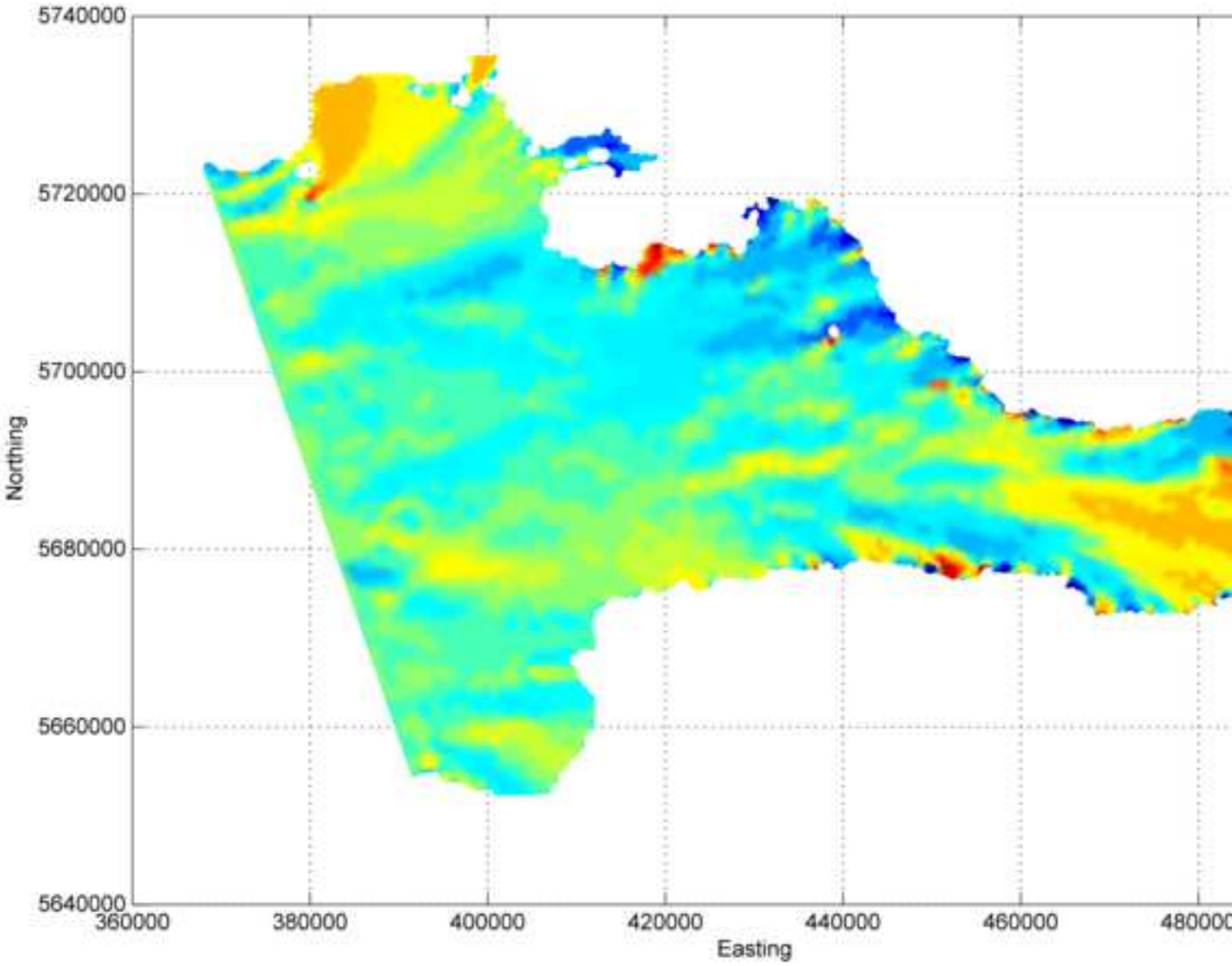

Figure 18
Click here to download high resolution image

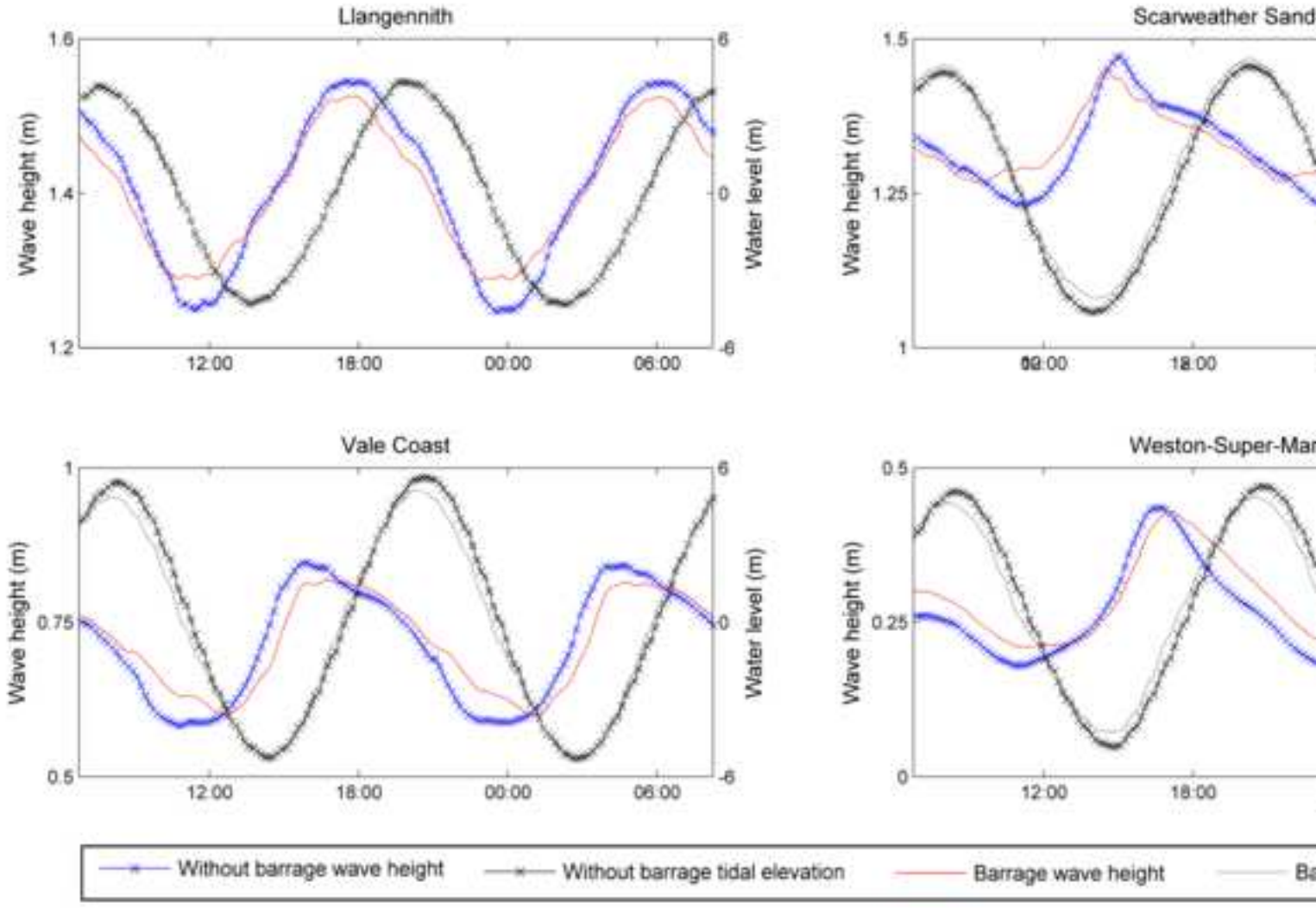

Figure 19
Click here to download high resolution image

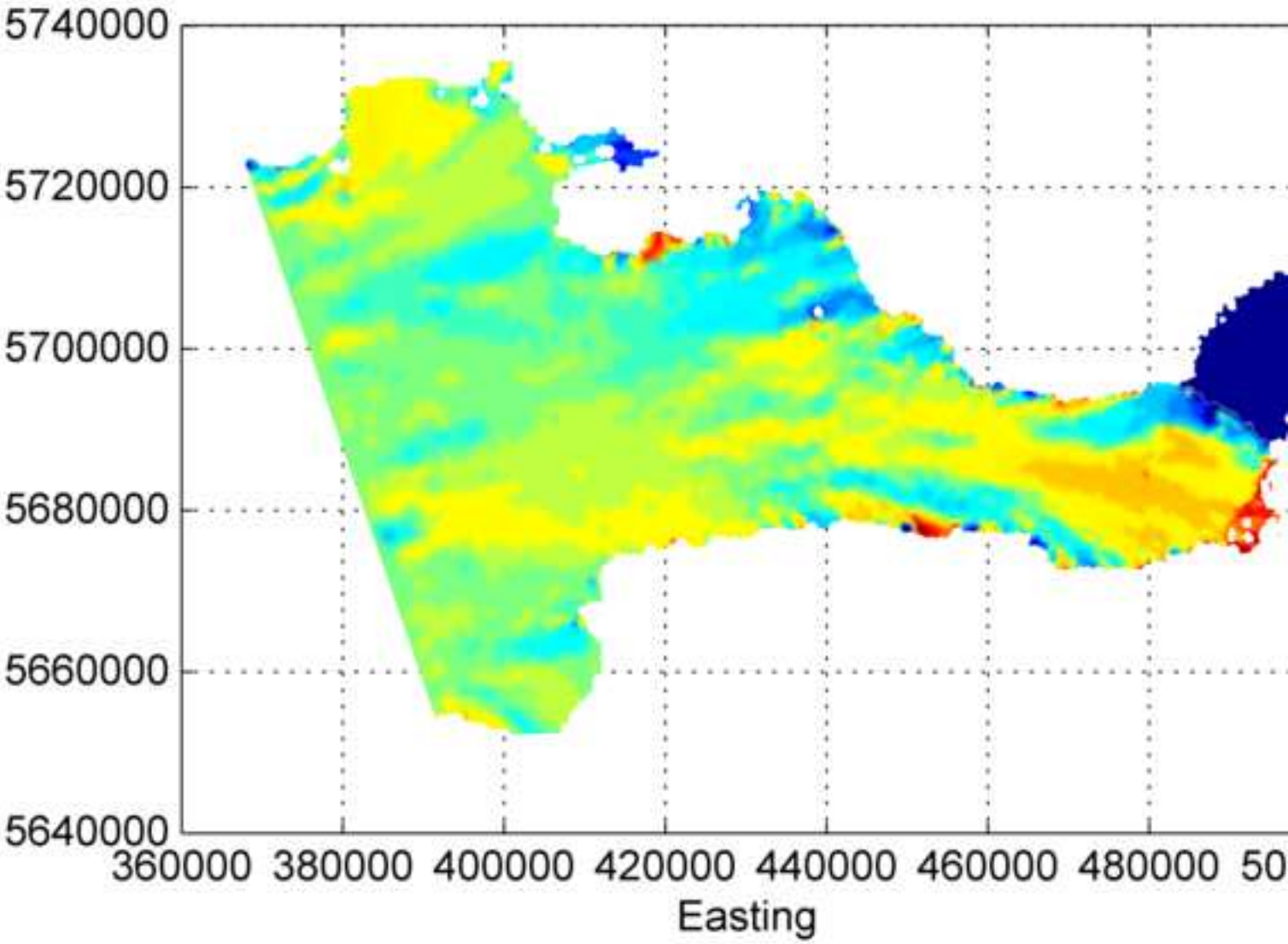
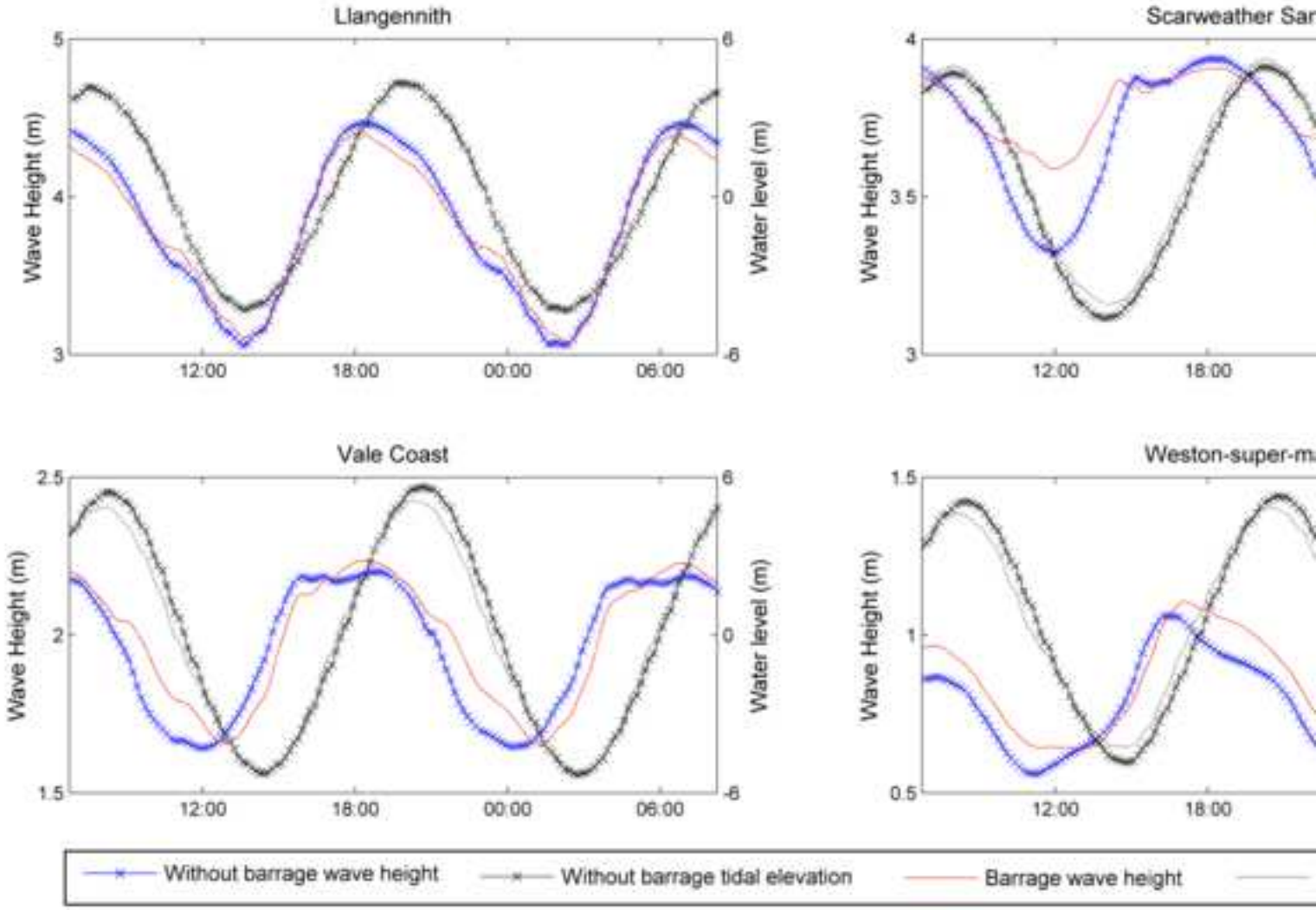
Figure 20
Click here to download high resolution image